Original Article

SHM Structural Health Monitoring

Structural Health Monitoring
1–25

DOI: 10.1177/14759217241264922
journals.sagepub.com/home/shm
Sage

An output-only damage identification method based on reinforcement-aided evolutionary algorithm and heterogeneous response reconstruction

Guangcai Zhang[1], Shuai Gao[1], Chunfeng Wan[1], Jianfei Kang[2], Liyu Xie[3] and Songtao Xue[3,4]

Abstract

The absence of excitation measurements may pose a huge challenge in the application of many damage identification methods since it is difficult to acquire the external excitations, such as wind load, traffic load. To deal with this issue, a novel output-only structural damage identification approach based on reinforcement-aided evolutionary algorithm and heterogeneous response reconstruction with Bayesian inference regularization is developed. On the one hand, heterogeneous measurements (e.g., displacements, strains, accelerations) are rescaled and reconstructed with the aid of Bayesian inference regularization technique. Structural damages are identified by minimizing the discrepancies between the measured and reconstructed responses. On the other hand, to solve the optimization-based inverse problem, a reinforcement-aided evolutionary algorithm, named Q-learning hybrid evolutionary algorithm (QHEA), integrating Jaya algorithm, differential algorithm, and Q-learning algorithm is proposed as search tool. To validate the feasibility and applicability of the proposed method, numerical studies on a three-span beam structure and laboratory tests on a five-story steel frame structure are carried out. The effects of data rescaling and data fusion on response reconstruction and damage identification are also investigated. The results clearly demonstrate the superiority of QHEA over other heuristic algorithms and heterogeneous data fusion over a single type of measurement. It is shown that both the locations and extents of the damaged elements can be accurately identified by the proposed method without the information of input force.

Keywords

Damage identification, output-only method, evolutionary algorithm, Q-learning, heterogeneous response reconstruction, data rescaling

Introduction

Civil structures may have performance degradation and damage accumulation during their long-term service period owing to various reasons, such as earthquakes, environmental corrosion, material aging, fatigue. It is significant to implement continuous health monitoring and early damage identification on the existing major infrastructure for the purposes of performance assessment, maintenance arrangement, future service life prediction, etc. Therefore, to evaluate the health status, various structural damage detection methods have been proposed over the past two decades.[1]

The vibration-based damage identification methods have been extensively investigated, and they can be

[1]Key Laboratory of Concrete and Prestressed Concrete Structure of Ministry of Education, Southeast University, Nanjing, China
[2]Graduate School of Engineering, Tohoku University, Sendai, Japan
[3]Department of Disaster Mitigation for Structures, Tongji University, Shanghai, China
[4]Department of Architecture, Tohoku Institute of Technology, Sendai, Japan

Jianfei Kang is now affiliated to School of Civil Engineering, Suzhou University of Science and Technology, Suzhou, China.

Corresponding authors:
Chunfeng Wan, Key Laboratory of Concrete and Pre-Stressed Concrete Structure of Ministry of Education, Southeast University, Sipailou 2#, Nanjing 210096, China.
Email: wan@seu.edu.cn

Songtao Xue, Department of Disaster Mitigation for Structures, Tongji University, Siping Road 1239#, Yangpu District, Shanghai 200092, China.
Email: xue@tongji.edu.cn

roughly divided into two categories, that is, frequency domain methods and time domain methods. Frequency domain methods utilize the changes in model parameters, such as frequencies,[2] mode shapes,[3] mode shape curvature,[4] modal strain energy,[5] and frequency response functions,[6] for structural damage identification especially in the case of unknown excitation, while some inherent drawbacks limit their practical engineering applications. It is found that low-order modes are easy to obtain, but they suffer from low sensitivity to minor or local damages. In comparison, high-order model information is more sensitive to small damages in principle but cannot be accurately extracted. For the latter category, some identification methods in time domain have been proposed directly using the time histories of dynamic responses recorded by sensors, such as the least-square method,[7] the maximum-likelihood estimation,[8] the extended Kalman filter,[9] the modified particle filter.[10] However, the requirement of excitation measurements may pose a huge challenge in the application of these damage identification methods since it is often difficult or even impossible to acquire external excitations, such as wind load, traffic load, earthquake. Notably, the unknown input excitation and local damages usually coexist. In this regard, output-only identification methods are more desirable.[11]

To address the absence of force measurement, the correlation function-based methods have been developed and received much attention. For example, Yang et al.[12] presented a cross correlation function amplitude vector to detect structure damage. Zhang et al.[13] successfully identified structural damages using heuristic algorithms and acceleration correlation functions when structure is subjected to ambient excitation. Although favorable results are achieved with correlation function-based methods, the requirement of long sampling duration and the assumption of stationary Gaussian white noise process restrict their application to some extent. Different from the aforementioned method, another type of output-only methods has been attempted, namely, simultaneous identification of both unknown structural damages and unmeasured input forces.[14] For instance, He et al.[15] and Zhang et al.[16] simultaneously identified structural parameters and external loads based on extended Kalman filter, and validated the effectiveness of the proposed method by a series of experimental tests, while it is noted that treating the unmeasured excitations as part of unknowns to be identified may further induce the ill-posedness of the identification problem. Kalman filter-based methods require initial estimate of the state vector and its covariance. Poor initial estimates can lead to slow convergence or divergence of the filter. This sensitivity to initial conditions can be a limitation in applications where accurate initial state estimates are not available. Besides, the need for matrix inversions and multiplications at each time step can pose significant computational demands, limiting the practical applicability of these approaches for large or complex structural systems. Jayalakshmi and Rao[17] adopted a new improved regularization method and dynamic hybrid adaptive firefly algorithm for simultaneous identification of input forces and system parameters. Zhang et al.[18] constructed an iterative strategy by combining Tikhonov regularization method for force identification and modified Jaya algorithm for damage identification.

In recent years, many investigators have reported the use of response reconstruction technique for the identification of structural damage, and fruitful results have been achieved.[19,20] Fan et al.[21] used densely connected convolutional networks to reconstruct acceleration responses of Guangzhou New Television Tower for the unavailable locations. Response reconstruction methods based on the transmissibility concept have received more and more attention, and their pleasant results in damage identification have been demonstrated in wavelet domain,[22] state space domain[23] and time domain.[24] In these proposed methods, the measured responses from the target structure are divided into two sets, denoted as measurement set 1 and measurement set 2. The responses of measurement set 2 can be reconstructed by using the transmissibility matrix and the first set of measurements. Structural damages are identified by minimizing the difference between the measured responses from real structure and reconstructed responses from the numerical model. In this way, structural damage identification in time domain is transformed into an optimization problem, solved by various heuristic algorithms, such as the particle swarm optimization,[25] the tree seeds algorithm,[26] the butterfly optimization algorithm,[27] the bat optimization algorithm.[28] Different from the abovementioned algorithms, a new swarm intelligence algorithm, named Jaya algorithm, was proposed by Rao in 2016 to solve diverse constrained and unconstrained benchmark problems.[29] The most distinct feature of Jaya algorithm is that any algorithm-specific parameters are not required. However, the poor search capability in the basic Jaya algorithm makes it face difficulties in dealing with complex optimization problems. Some modifications have been presented in previous studies, introducing search space reduction method,[30] k-means clustering,[31] Hooke–Jeeves pattern search,[32] shuffling process,[33] etc. However, it is noted that the search mode in these abovementioned algorithms is still relatively single and monotonous, which is difficult to achieve good balance between the exploration and the exploitation. Inspired by the idea that different search strategies have different optimization performances, to solve the drawback of single search mode, in this

paper, a novel reinforcement-aided evolutionary algorithm, named Q-learning hybrid evolutionary algorithm (QHEA), is proposed by integrating Jaya algorithm, differential evolutionary (DE) algorithm, and Q-learning algorithm. In each iteration, the best search strategy from Jaya or DE is adaptively selected under the guidance of Q-learning. To this end, the balance between the exploration and exploitation of QHEA is well achieved.

Nevertheless, most of the output-only methods for damage identification problem in the present literature only use a single type of measurement. From the practical point of view, nowadays, multi-type sensors, such as displacement transducers, strain gauges, accelerometers are widely employed in the structural health monitoring systems of large-scale civil structures. Some studies have reported that making full use of heterogeneous responses can enhance the accuracy and reliability of damage detection.[34] For example, Zhao et al.[35] proposed a nonlinear restoring forces identification scheme through multisensor data fusion of accelerometers and displacement responses, and the results showed the superiority of hybrid sensor measurement. Zhang and Xu[36] presented a multisensing damage identification method via response reconstruction, and verified the effectiveness of the proposed method with laboratory tests on a simply supported overhanging beam. Jeong et al.[37] applied hybrid acceleration and angular velocity to successfully identify damages of monopile offshore wind turbine structures. Wang et al.[38] developed a damage detection method based on the cross-correlation function among acceleration and strain data. Based on these previous studies, it is found that different types of sensors, accelerometers, strain gauges, and displacement transducers, etc., have their own merits and drawbacks. Therefore, heterogeneous response reconstruction is suggested for output-only damage identification.

Considering the necessities of developing output-only damage identification for civil structures under unknown excitation, feasibilities of swam intelligent algorithms and reinforcement algorithm in solving the optimization-based inverse problem with multitype structural responses in practice, in this study, an iterative strategy to identify the unknown structural damages using output-only fused incomplete dynamic response measurements is proposed. The contribution of the present paper is that an output-only structural damage identification based on QHEA and heterogeneous response reconstruction with Bayesian inference regularization is proposed, to deal with the problem of structural damage identification without the input excitation. First, heterogeneous response reconstruction technique is derived considering the complementary benefits of multitype sensors. Additionally, to solve the ill-posed problem in response reconstruction owing to the presence of measurement noise, Bayesian inference regularization is adopted, and the drifted estimation of external excitation and structural responses can be properly addressed. Moreover, to optimize the objective function established based on the measured and reconstructed responses, a new reinforcement-aided evolutionary algorithm QHEA is proposed by integrating the Jaya, DE and Q-learning algorithms. The global search capability of evolutionary algorithms and the adaptive learning ability of reinforcement learning are combined. This adaptive nature of QHEA enhances its robustness and scalability, making it well-suited to tackle high-dimensional optimization problems, providing a more reliable solution for structural damage identification. Finally, numerical studies on a 40-element three-span beam structure and experimental validations on a five-floor steel frame structure are conducted to demonstrate the applicability of the proposed method. The effects of measurement noise, modeling error, data rescaling, data fusion on the identification results are also investigated.

Heterogeneous response reconstruction

Response reconstruction in time domain

The equation of motion of a linear structural system subjected to external input force can be expressed as follows:

$$M\ddot{u}(t) + C\dot{u}(t) + Ku(t) = Bf(t) \tag{1}$$

where $\ddot{u}(t)$, $\dot{u}(t)$, $u(t)$ stand for the vectors of acceleration, velocity, and displacement responses, respectively; M, C, K are the mass, damping, stiffness matrices; $f(t)$ means the time-dependent external excitation and B denotes the mapping matrix with the value of 1 relating the force location. Rayleigh damping model[30] $C = aM + bK$ is adopted.

For a structure under the unit impulse excitation, the motion equation can be written as

$$M\ddot{h}(t) + C\dot{h}(t) + Kh(t) = B\delta(t) \tag{2}$$

where $\delta(t)$ is the Dirac delta function. The impulse response function is able to be represented as a free vibration state with the specific initial conditions.[39] Assuming the structural system is initially in static equilibrium, the unit impulse response function can be calculated by numerical integration methods, for example, Newmark-β method

$$\begin{cases} M\ddot{h}(t) + C\dot{h}(t) + Kh(t) = 0 \\ h(0) = 0, \dot{h}(0) = M^{-1}B \end{cases} \tag{3}$$

where $h(t)$, $\dot{h}(t)$, $\ddot{h}(t)$ are the unit impulse displacement, velocity, and acceleration vectors in the time domain, respectively.

The strain responses $\varepsilon_q(t_n)$ at the location q with local co-ordinates (x, y) in a typical Euler beam element can be described[40]

$$\varepsilon_q = \frac{u_j^* - u_i^*}{l} + \left(\frac{6y}{l^2} - \frac{12xy}{l^3}\right)v_i^* + \left(\frac{4y}{l} - \frac{6xy}{l^2}\right)\theta_i^* + \left(-\frac{6y}{l^2} + \frac{12xy}{l^3}\right)v_j^* + \left(\frac{2y}{l} - \frac{6xy}{l^2}\right)\theta_j^* \tag{4}$$

where $\left[u_i^*, v_i^*, \theta_i^*, u_j^*, v_j^*, \theta_j^*\right]^T$ stand for the i-th and j-th nodal displacement vectors of the e-th element; l means the length of element.

The degrees of freedom (DOFs) of elemental nodal displacements $u_i^*, v_i^*, \theta_i^*, u_j^*, v_j^*, \theta_j^*$ is rewritten as $e1$, $e2$, $e3$, $e4$, $e5$, $e6$. The unit strain impulse response function $h_q^{\varepsilon}(t)$ at location q can be calculated by the unit displacement impulse response function

$$h_q^{\varepsilon}(t) = \frac{h_{e4}(t) - h_{e1}(t)}{l} + \left(\frac{6y}{l^2} - \frac{12xy}{l^3}\right)h_{e2}(t) + \left(\frac{4y}{l} - \frac{6xy}{l^2}\right)h_{e3}(t) + \left(-\frac{6y}{l^2} + \frac{12xy}{l^3}\right)h_{e5}(t) + \left(\frac{2y}{l} - \frac{6xy}{l^2}\right)h_{e6}(t) \tag{5}$$

where $h_{e1}(t), h_{e2}(t), h_{e3}(t), h_{e4}(t), h_{e5}(t), h_{e6}(t)$ are the unit displacement impulse response function for the DOFs $e1$, $e2$, $e3$, $e4$, $e5$, $e6$, respectively.

For a structural system with zero initial conditions, the displacement, strain, and acceleration responses from the m-th, q-th, s-th DOFs at instant t_n under general external excitation $f(t)$ can be expressed as Equations (6)–(8), respectively,

$$u_m(t_n) = \int_0^{t_n} h_m(t_n - \tau)f(\tau)\mathrm{d}\tau \tag{6}$$

$$\varepsilon_q(t_n) = \int_0^{t_n} h_q^{\varepsilon}(t_n - \tau)f(\tau)\mathrm{d}\tau \tag{7}$$

$$\ddot{u}_s(t_n) = \int_0^{t_n} \ddot{h}_s(t_n - \tau)f(\tau)\mathrm{d}\tau \tag{8}$$

where $u_m(t_n)$, $\varepsilon_q(t_n)$, $\ddot{u}_s(t_n)$ are the displacement, strain, and acceleration measurements; $h_m(t_n - \tau)$, $h_q^{\varepsilon}(t_n - \tau)$, $\ddot{h}_s(t_n - \tau)$ denote the unit displacement, strain, acceleration impulse response functions, respectively.

The discrete form of Equations (6)–(8) can be expressed as Zhang et al.[13]

$$u_m(t_n) = \sum_{\tau=0}^{t_n} h_m(t_n - \tau)f(\tau) \tag{9}$$

$$\varepsilon_q(t_n) = \sum_{\tau=0}^{t_n} h_q^{\varepsilon}(t_n - \tau)f(\tau) \tag{10}$$

$$\ddot{u}_s(t_n) = \sum_{\tau=0}^{t_n} \ddot{h}_s(t_n - \tau)f(\tau) \tag{11}$$

The relationship between the output responses and input force can be written as

$$Y_u = H_u F,\ Y_{\varepsilon} = H_{\varepsilon} F,\ Y_{\ddot{u}} = H_{\ddot{u}} F \tag{12}$$

where Y_u, Y_{ε}, $Y_{\ddot{u}}$ are the assembled displacement, strain, and acceleration measurements, $Y_u = [y_{u_1}, y_{u_2}, ..., y_{u_n}]^T$, $Y_{\varepsilon} = [y_{\varepsilon_1}, y_{\varepsilon_2}, ..., y_{\varepsilon_n}]^T$, $Y_{\ddot{u}} = [y_{\ddot{u}1}, y_{\ddot{u}2}, \ldots, y_{\ddot{u}n}]^T$. The dimensions of Y_u, Y_{ε}, $Y_{\ddot{u}}$ are $(u_n \times t_n) \times 1$, $(\varepsilon_n \times t_n) \times 1$, $(\ddot{u}_n \times t_n) \times 1$, and u_n, ε_n, $\ddot{u}_n$ represent the number of displacement sensors, strain gauges, accelerometers. The dimension of external excitation F is $t_n \times 1$.

In Equation (12), $H_u = [H_{u_1}, H_{u_2}, ..., H_{u_n}]^T$, $H_{\varepsilon} = [H_{\varepsilon_1}, H_{\varepsilon_2}, ..., H_{\varepsilon_n}]^T$, $H_{\ddot{u}} = [H_{\ddot{u}1}, H_{\ddot{u}2}, \ldots, H_{\ddot{u}n}]^T$, the dimensions of H_u, H_{ε}, $H_{\ddot{u}}$ are $(u_n \times t_n) \times t_n$, $(\varepsilon_n \times t_n) \times t_n$, $(\ddot{u}_n \times t_n) \times t_n$, and they can be given by following equations, respectively

$$H_u = \begin{bmatrix} h_{u_n}(t_0) & 0 & 0 & 0 & 0 \\ h_{u_n}(t_1) & h_{u_n}(t_0) & 0 & 0 & 0 \\ h_{u_n}(t_2) & h_{u_n}(t_1) & h_{u_n}(t_0) & 0 & 0 \\ \vdots & \vdots & \vdots & \ddots & \vdots \\ h_{u_n}(t_n) & h_{u_n}(t_{n-1}) & h_{u_n}(t_{n-2}) & \cdots & h_{u_n}(t_0) \end{bmatrix} \tag{13}$$

$$H_{\varepsilon} = \begin{bmatrix} h_{\varepsilon_n}^{\varepsilon}(t_0) & 0 & 0 & 0 & 0 \\ h_{\varepsilon_n}^{\varepsilon}(t_1) & h_{\varepsilon_n}^{\varepsilon}(t_0) & 0 & 0 & 0 \\ h_{\varepsilon_n}^{\varepsilon}(t_2) & h_{\varepsilon_n}^{\varepsilon}(t_1) & h_{\varepsilon_n}^{\varepsilon}(t_0) & 0 & 0 \\ \vdots & \vdots & \vdots & \ddots & \vdots \\ h_{\varepsilon_n}^{\varepsilon}(t_n) & h_{\varepsilon_n}^{\varepsilon}(t_{n-1}) & h_{\varepsilon_n}^{\varepsilon}(t_{n-2}) & \cdots & h_{\varepsilon_n}^{\varepsilon}(t_0) \end{bmatrix} \tag{14}$$

$$H_{\ddot{u}} = \begin{bmatrix} \ddot{h}_{\ddot{u}_n}(t_0) & 0 & 0 & 0 & 0 \\ \ddot{h}_{\ddot{u}_n}(t_1) & \ddot{h}_{\ddot{u}_n}(t_0) & 0 & 0 & 0 \\ \ddot{h}_{\ddot{u}_n}(t_2) & \ddot{h}_{\ddot{u}_n}(t_1) & \ddot{h}_{\ddot{u}_n}(t_0) & 0 & 0 \\ \vdots & \vdots & \vdots & \ddots & \vdots \\ \ddot{h}_{\ddot{u}_n}(t_n) & \ddot{h}_{\ddot{u}_n}(t_{n-1}) & \ddot{h}_{\ddot{u}_n}(t_{n-2}) & \cdots & \ddot{h}_{\ddot{u}_n}(t_0) \end{bmatrix} \tag{15}$$

It is noted that the magnitudes of heterogeneous measurements, such as displacement, strain, and acceleration are very different, so rescaling coefficients are introduced into Equation (12) as follows:

$$\tilde{Y}_u = a_u Y_u = a_u H_u F = \tilde{H}_u F$$
$$\tilde{Y}_\varepsilon = a_\varepsilon Y_\varepsilon = a_\varepsilon H_\varepsilon F = \tilde{H}_\varepsilon F$$
$$\tilde{Y}_{\ddot{u}} = a_{\ddot{u}} Y_{\ddot{u}} = a_{\ddot{u}} H_{\ddot{u}} F = \tilde{H}_{\ddot{u}} F \quad (16)$$

where a_u, a_ε, $a_{\ddot{u}}$ are the rescaling coefficients, and they can be calculated by

$$a_u = \|Y_u\|_2^{-1},\ a_\varepsilon = \|Y_\varepsilon\|_2^{-1},\ a_{\ddot{u}} = Y_{\ddot{u}2}^{-1} \quad (17)$$

where $\|\ \|_2$ represents the L_2 norm of the given vector.

The heterogeneous data fusion can be achieved by

$$Y = HF \quad (18)$$

where $Y = \left[\tilde{Y}_u, \tilde{Y}_\varepsilon, \tilde{Y}_{\ddot{u}}\right]^T$, $H = \left[\tilde{H}_u, \tilde{H}_\varepsilon, \tilde{H}_{\ddot{u}}\right]^T$, $\tilde{H}_u = a_u H_u$, $\tilde{H}_\varepsilon = a_\varepsilon H_\varepsilon$, $\tilde{H}_{\ddot{u}} = a_{\ddot{u}} H_{\ddot{u}}$.

In previous studies, response reconstruction technique has been applied into output-only structural identification with only one type of sensor. In practice, a multisensors monitoring system is usually installed on the large infrastructure, thus heterogeneous measurements, displacements, strains, accelerations, etc., are available. Herein, response reconstruction with multiple types of vibration data in time domain is derived. First, heterogeneous responses can be divided into two sets, that is, measurement set 1 Y_{mea}^{set1} and set 2 Y_{mea}^{set2}, given by

$$\begin{cases} Y_{mea}^{set1} = H_1 F \\ Y_{mea}^{set2} = H_2 F \end{cases} \quad (19)$$

It is noted that there is no specific rule about how to divide the multitype responses into two sets, but the number of sensors in the measurement set 1 should exceed the number of unknown external excitations on the structure.

Then, the unknown input force and dynamic responses of the second set can be calculated using the first set of measurements as follows:

$$F = (H_1)^+ Y_{mea}^{set1} \quad (20)$$
$$Y_{rec}^{set2} = H_2 (H_1)^+ Y_{mea}^{set1} \quad (21)$$

where $()^+$ means the pseudoinverse and transformation matrix $T_{12} = H_2 (H_1)^+$.

For Equations (20) and (21), the ordinary least squares may lead to unbounded solution especially taking the noise-polluted measurements into consideration. In order to deal with the misidentified estimation of external excitation and responses, Tikhonov regularization method[41] is employed

$$F = \left(H_1{}^T H_1 + \lambda I\right)^{-1} H_1^T Y_{mea}^{set1} \quad (22)$$
$$Y_{rec}^{set2} = T_{12} Y_{mea}^{set1} = H_2 \left(H_1^T H_1 + \lambda I\right)^{-1} H_1^T Y_{mea}^{set1} \quad (23)$$

where λ stands for the nonnegative regularization parameter; I means the identity matrix.

As is known, the key point of using Tikhonov regularization technique lies in how to efficiently find the optimal regularization parameter λ. The L-curve method, the generalized cross-validation method, and the S-curve method have been adopted but suffer from comparatively expensive computation issue for a large-scale matrix. In addition, it may find that the L-curve doesn't have a distinct corner, leading to the difficulty in determining the regularization parameter. In recent years, Bayesian inference method has been developed to adaptively determine the regularization parameter, adopted in this study.

Bayesian inference method

In this section, a statistical Bayesian learning scheme is used to reconstruct the unknown input force. The unknown force F is modeled in the posterior probability density function (PDF) $p(F, \sigma^2, \tau^2 | Y)$ through hierarchical modeling as follows[42]:

$$p\left(F, \sigma^2, \tau^2 | Y\right) \propto p\left(Y | F, \sigma^2\right) p\left(F | \tau^2\right) p\left(\sigma^2\right) p\left(\tau^2\right) \quad (24)$$

where $p(Y|F, \sigma^2)$ means the likelihood function and $p\left(F|\tau^2\right)$ represents the prior PDF, and they can be expressed as

$$p\left(Y | F, \sigma^2\right) \propto \frac{1}{\sigma^{n_0 N}} \exp\left(-\frac{1}{2\sigma^2} \|HF - Y\|^2\right) \quad (25)$$

$$p\left(F|\tau^2\right) \propto \frac{1}{\tau^{n_f N}} \exp\left(-\frac{1}{2\tau^2} \|F\|^2\right) \quad (26)$$

where n_0 means the total number of measurements including displacements, strains, and accelerations, that is, $n_0 = u_n + \varepsilon_n + \ddot{u}_n$; σ and τ stand for the standard deviation and scaling parameter; n_f represents the number of force.

For the hyperparameters σ^2 and τ^2, $p(\sigma^2)$ and $p(\tau^2)$ are their conjugate prior PDFs, modeled as the following inverse Gamma distribution[42]

$$p\left(\sigma^2\right) = \frac{{b_1}^{a_1}}{\Gamma(a_1)} \sigma^{-2(a_1+1)} e^{-b_1 \sigma^{-2}},$$
$$p\left(\tau^2\right) = \frac{{b_2}^{a_2}}{\Gamma(a_2)} \tau^{-2(a_2+1)} e^{-b_2 \tau^{-2}} \quad (27)$$

where a_1, b_1, a_2, b_2 denote the nonnegative hyperparameters.

The posterior PDF is written as

$$p(F,\sigma^2,\tau^2|Y)\propto\frac{\tau^{-2(a_2+1)-n_fN}}{\sigma^{2(a_1+1)+n_0N}}\exp\left(-\frac{1}{2\sigma^2}\|HF-Y\|^2-\frac{1}{2\tau^2}\|F\|^2-b_1\sigma^{-2}-b_2\tau^{-2}\right) \tag{28}$$

By the logarithm and the negative of Equation (28), the following equation is obtained

$$J(F,\sigma^2,\tau^2)=\frac{1}{2\sigma^2}\|HF-Y\|^2+\frac{1}{2\tau^2}\|F\|^2+b_1\sigma^{-2}+b_2\tau^{-2}+\left[2(a_2+1)+n_fN\right]\ln\tau+\left[2(a_1+1)+n_0N\right]\ln\sigma \tag{29}$$

Setting the partial derivative of $J(F,\sigma^2,\tau^2)$ to zero. The optimal solutions $\hat{F}$ can be obtained by

$$\hat{F}=\left(H^TH+\frac{\hat{\sigma}^2}{\hat{\tau}^2}I\right)^{-1}H^TY \tag{30}$$

The regularization parameter can be automatically determined by $\lambda=\frac{\hat{\sigma}^2}{\hat{\tau}^2}$, then, the unmeasured input force is reconstructed.

Reinforcement-aided evolutionary algorithm

In this section, damage identification problem is transformed into a nonlinear optimization-based inverse problem. The objective function is first given, and then a new reinforcement-aided evolutionary algorithm QHEA is proposed to solve this optimization problem.

Optimization-based damage identification problem

As presented in Refs. 18, 21, 22, 31, and 32, structural damage is simulated as linear reduction of flexural stiffness and the alternation of mass matrix is directly ignored. Assuming the target structure consists of *ne* elements, the damage extent of the *i*-th element can be defined as

$$\alpha_i=\frac{E_i-E_i^d}{E_i},\quad i=1,2,\ldots ne \tag{31}$$

where α_i denotes the *i*-th elemental damage extent; ne means the number of elements; E_i and E_i^d stand for the elasticity modulus of element *i* in the healthy state and damaged state, respectively.

The damaged structural stiffness matrix K^d can be expressed as

$$K^d=\sum_{i=1}^{ne}(1-\alpha_i)K_i^{ele},\ 0\leqslant\alpha_i\leqslant1 \tag{32}$$

where K_i^{ele} stands for the *i*-th elemental stiffness matrix under the healthy state; ne means the number of total elements. It is noted that $\alpha_i=0$ denotes the *i*-th element is intact while $\alpha_i=1$ implies the *i*-th element is completely damaged.

The acceleration responses are utilized to establish the objective function owing to their abundant information relevant to structural damages. In the optimization-based damage identification problem, the purpose is to find the best structural parameters θ by minimizing the discrepancy between the measured responses Y_{mea}^{set2} and the reconstructed responses $Y_{rec}^{set2}(\theta)$ of the second set from the damaged structure as follows:

$$obj=\left\|Y_{mea}^{set2}-Y_{rec}^{set2}(\theta)\right\|_2 \tag{33}$$

where *obj* represents the objective function to be optimized; the unknown structural parameter is calculated by $\theta_i=1-\alpha_i$ within the range of [0, 1].

Q-learning hybrid evolutionary algorithm

In this section, a novel QHEA is proposed as search tool in damage identification. A search strategy pool is formulated based on Jaya algorithm and differential evolution algorithm, and the best strategy will be adaptively selected for each individual under the guidance of Q-learning algorithm.

Search strategy pool. DE and Jaya algorithm belong to the population-based stochastic optimization algorithms. Each individual in the population represents a candidate solution of structural damage index vector. The initial population can be randomly generated within the upper and lower search limits.[30]

For DE or Jaya algorithm, exploration and exploitation are two necessary components to guide the direction of heuristic algorithm, while there is a paradox between global exploration and local exploitation. The former refers to exploring the new regions in the given search space, whereas the latter implies accessing the areas around the previously visited points. If DE or Jaya algorithm focuses on the global exploration mode excessively, the convergence performance would be weakened to some extent. In contrast, if much attention is paid to the local exploitation mode, the algorithm might fall into local optimum. Therefore, to achieve the trade-off between exploitation and exploration, a search strategy pool including DE/rand/1 and DE/rand/2, DE/current-to-best/1 and Jaya mutation is developed by combining the merits of different search strategies, given by

$$Strategy\ pool = \begin{cases} Group_1 \begin{cases} DE/rand/1 \\ DE/rand/2 \end{cases} \\ Group_2 \begin{cases} DE/current-to-best/1 \\ Jaya\ mutation \end{cases} \end{cases} \tag{34}$$

Strategy pool represents a repository including several different search operations. By Equation (34), the proposed search strategy pool has two different groups, that is, $Group_1$ and $Group_2$. $Group_1$ consists of two commonly referred mutation strategies of DE/rand/1 and DE/rand/2, denoted as exploration group, and $Group_2$ contains two different strategies, namely, DE/current-to-best/1 and Jaya mutation, denoted as exploitation group. Search strategy pool can be further expressed as

$$Strategy\ pool = \begin{cases} V_{i,G} = X_{r_1,G} + F_{mu}(X_{r_2,G} - X_{r_3,G}) \\ V_{i,G} = X_{r_1,G} + F_{mu}(X_{r_2,G} - X_{r_3,G}) + F_{mu}(X_{r_4,G} - X_{r_5,G}) \\ V_{i,G} = X_{i,G} + F_{mu}(X_{best,G} - X_{i,G}) + F_{mu}(X_{r_1,G} - X_{r_2,G}) \\ V_{i,j,G} = X_{i,j,G} + rand_1 \times \left(X_{best,j,G} - \left|X_{i,j,G}\right|\right) - rand_2 \times \left(X_{worst,j,G} - \left|X_{i,j,G}\right|\right) \end{cases} \tag{35}$$

where $X_{r_1,G}, X_{r_2,G}, X_{r_3,G}, X_{r_4,G}, X_{r_5,G}$ stand for five different candidate solutions randomly selected from the current population at the G-th iteration, and it is noted $r_1 \neq r_2 \neq r_3 \neq r_4 \neq r_5 \neq i$; F_{mu} represents the mutation operator, set as 0.8; $rand_1$ and $rand_1$ are two random numbers in the range of [0, 1]; $V_{i,G}$ is the i-th mutated individual; $X_{best,j,G}$ and $X_{worst,j,G}$ mean the value of the j-th variable for the best and the worst individuals at the G-th iteration, respectively; $\left|X_{i,j,G}\right|$ denotes the absolute value of $X_{i,j,G}$.

By Equation (34), it is found that the search strategy pool combines the strong global exploration capacity of $Group_1$ and the powerful local exploitation capacity of $Group_2$, so the tradeoff between exploration and exploitation can be better realized.

Q-learning algorithm. Reinforcement learning as a representative kind of machine learning technique aims to make the agent take the optimal action under an unknown environment so as to get the maximum long-term rewards. Q-learning is one of the most classical and well-known algorithms of reinforcement learning that recently has been widely utilized to improve the performance of diverse heuristic algorithms, such as simulated annealing,[43] tree seeds algorithms,[44] water strider algorithm.[45] There are five main components of Q-learning algorithm, namely, learning agent, an environment, states, actions, and rewards. More detailed description can be found in Huynh et al.[46]

To implement the Q-learning algorithm, a set of states of the environment $S = \{s_1, s_2, ..., s_n\}$ and corresponding actions $A = \{a_1, a_2, ..., a_n\}$ to be performed for the learning agent are considered. During the iterative learning process, the target agent determines the probability of choosing different actions in different states according to the Q-table. The updating Bellman equation of Q-value is given as follows:

$$Q^{new}(s_t, a_t) = (1 - \varphi)Q(s_t, a_t) + \varphi[w_{t+1} + \gamma \cdot \max Q(s_{t+1}, a_t)] \tag{36}$$

where $Q(s_t, a_t)$ and $Q^{new}(s_t, a_t)$ stand for the previous and new Q-values; $\max Q(s_{t+1}, a_t)$ denotes the maximum Q-value for all actions; φ means the learning rate within [0, 1]; γ represents the discount factor within [0, 1]; w_{t+1} refers to the observed reward/penalty obtained from executing action a.

The discount factor γ determines the effect of the future reward on the agent decisions, usually set as 0.8. To make the Q-learning switch from more exploration to exploitation mode, the learning rate φ is set as $\varphi_t = 1 - 0.9 \times \frac{Iter}{Max\_Iter}$,[46] in which Iter and Max_Iter are the current iteration number and the maximum iteration numbers.

Implementation of QHEA. Inspired by abundant successful applications of Q-learning in heuristic algorithms, herein, QHEA is proposed by integrating the search strategy pool and the Q-learning together. Specifically, the individuals of optimization algorithms act as the learning agent; the environment refers to the search domain of the individuals; the states represent the current operation of each individual, that is, DE/rand/1, DE/rand/2, DE/current-to-best/1 and Jaya mutation; the action stands for it changes from one state to another.

The proposed QHEA can be carried out as following several steps. Initially, the initial population of hybrid algorithm is randomly generated. Then, randomly produce a 4×4 matrix $Q(s_t, a_t)$ as the initial Q-table for each individual in the current population. The dimension of matrix Q is the number of search strategies. Next, the individual selects the best operation on the basis of the position of the maximum Q-value in the Q-table as follows:

$$best\ action = Max[Q(current\ state,\ all\ actions)] \tag{37}$$

Subsequently, for the current individual, implement the selected operation and calculate the new objective

Define the population size NP, dimension of parameter Dim, maximum number of iterations Max_Iter, mutation operator F_{mu} and crossover operator CR, the upper and lower search space limits
Randomly generate an initial population within the predefined search space
Randomly produced a 4×4 matrix Q as initial Q-table
Initialize iteration number $Iter = 1$
While termination criterion is not reached **do**
  For every individual X_i in the population
    Calculate the objective function value
    Find the best individual and the worst one in the current population
  Select the best action a_t for the current state s_t according to the Q-table value
    Switch action
      Case 1
        Update solution with DE/rand/1
    Case 2
        Update solution with DE/rand/2
    Case 3
        Update solution with DE/current-to-best/1
      Case 4
        Update solution with Jaya mutation
  End for
  Implement crossover operation
  Evaluate the objective function of updated individuals
  For individual $i = 1$ to NP
   Individual with better solution will survive according to greedy selection mechanism
   Obtain the immediate reward based on Eq. (32)
   Determine the maximum Q-value for the next state s_{t+1}
   Update the Q-table with Eq. (30) and update the current state $s_t = s_{t+1}$
  End for
  $Iter = Iter + 1$
End while
Output the identified best solution and its optimal value

Figure 1. The pseudocode of proposed QHEA.
QHEA: Q-learning hybrid evolutionary algorithm.

function. The positive reward and negative penalty are defined according to whether the objective function is improved

$$w_t = \begin{cases} 1 & \textit{if obj} \text{ is improved} \\ -1 & \textit{otherwise} \end{cases} \tag{38}$$

Update the content of Q-table with Equations (36). Finally, repeat iteration process until termination criterion is reached. The pseudocode of the proposed QHEA is presented in Figure 1.

The proposed QHEA effectively combines the merits of different search strategies, that is, DE/rand/1, DE/rand/2, DE/current-to-best/1 and Jaya mutation in the framework of Q-learning algorithm. For each individual, the most suitable search strategy is adaptively selected. To this end, the balance between the exploration and exploitation of QHEA is effectively achieved.

Implementation procedures

In this section, an iterative strategy is developed to identify the unknown structural damages with the incomplete output-only responses, and its flowchart is shown in Figure 2. The measured multiple types of dynamic responses, including displacements, strains, accelerations, are divided into two different measurement sets, that is, measurement set 1 Y_{mea}^{set1} and measurement set 2 Y_{mea}^{set2}. As presented in Figure 2, measurement set 1 is utilized to reconstruct unmeasured input force based on Bayesian inference regularization method while measurement set 2 is employed to construct the objective function to be optimized by the proposed QHEA. The structural damages and the unknown external excitation can be iteratively estimated by minimizing the objective function defined in Equation (33) until the termination criterion is satisfied.

Herein, more detailed implementation procedures of the proposed method are illustrated as follows:

Step 1: Predefine parameters of QHEA including population size NP, dimension of parameter Dim, maximum number of iterations Max_Iter, mutation operator F_{mu} and crossover operator CR; randomly produce initial guess of structural parameters θ within upper and lower search space limits as the starting point for the optimization process.

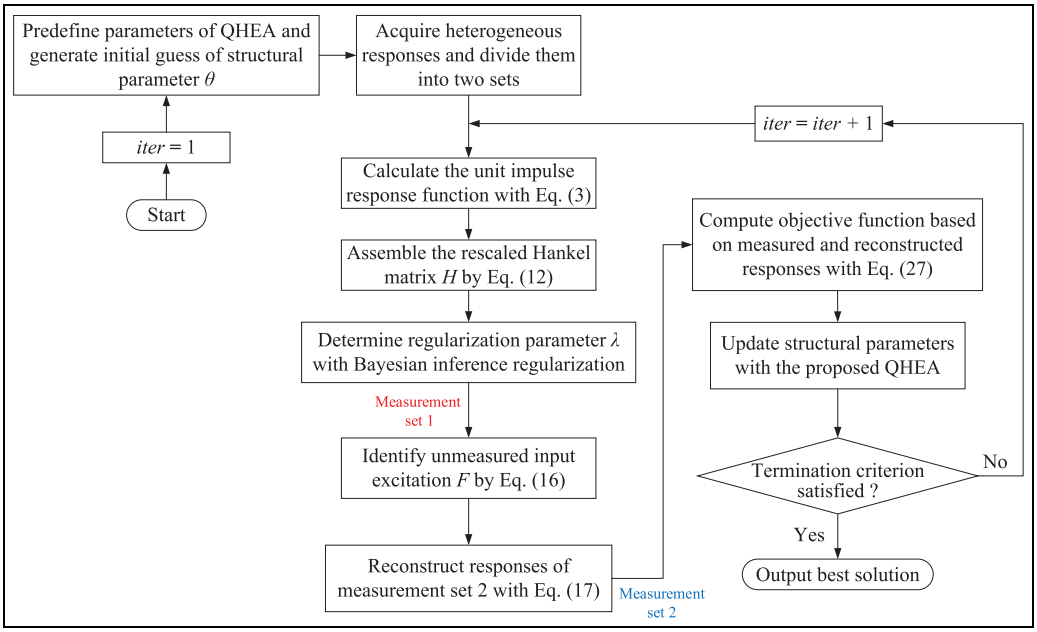

Figure 2. Implementation procedures of proposed identification method.

Step 2: Acquire the dynamic heterogeneous responses including displacements, strains, accelerations from the damaged structure; rescale these measurements and divide them into two different measurement sets, that is, set 1 Y_{mea}^{set1} and set 2 Y_{mea}^{set2}.

Step 3: Calculate the unit impulse displacement, velocity, and acceleration vectors using Equation (3) and obtain Hankel matrices H_u, H_ε, $H_{\ddot{u}}$ with Equations (13)–(15); compute the rescaling coefficients a_u, a_ε, $a_{\ddot{u}}$ by Equation (17) and assemble the rescaled matrices $H = \left[\tilde{H}_u, \tilde{H}_\varepsilon, \tilde{H}_{\ddot{u}}\right]^T$ in Equation (18).

Step 4: Set small hyperparameters for the Bayesian inference-based regularization parameter a_1, b_1, a_2, b_2; determine regularization parameter λ with Bayesian inference regularization, identify the unmeasured input force with Equation (22), and reconstruct responses of measurement set 2 Y_{rec}^{set2} using Equation (23).

Step 5: Construct the objective function using Equation (33) based on the measured responses Y_{mea}^{set2} and the reconstructed responses Y_{rec}^{set2} of measurement set 2 from the damaged structure.

Step 6: Optimize the objective function by iteratively updating structural parameters θ_{iter} with the proposed QHEA.

Step 7: Repeat steps 3–6 until the maximum iteration numbers are reached or convergence criteria is satisfied as follows:

$$\frac{\|\theta_{i,\,iter+1} - \theta_{i,\,iter}\|_2}{\|\theta_{i,\,iter}\|_2} \times 100\% \leqslant Tolerance \qquad (39)$$

where *Tolerance* stands for the convergence tolerance value.

Step 8: Output the identified external excitation and structural damages.

Numerical studies

To verify the applicability and effectiveness of the proposed output-only identification method, numerical studies on a three-span beam structure are conducted in MATLAB 2020a on the Intel(R) Core i5-13600 CPU @ 3.50 GHz PC with 16.00 GB RAM. The statistical results from 20 independent runs are summarized as the final results.

The numerical model of three-span beam structure is shown in Figure 3. It is observed that the beam structure is numerically modeled by 40 Euler–Bernoulli elements, and the length of each element is 100 mm. The width and height of the rectangular cross-section are 50 and 6 mm, respectively. There is a pin support at the node 11 and a roller support at the node 31. For the steel material of the beam elements, the Young's modulus and mass density are 2.1×10^{11} N/m^2 and 7860 kg/m^3, respectively. The Rayleigh damping model is adopted, and the damping ratio is set as 1% for the first two modes to determine the coefficients. The first ten natural frequencies are 1.9, 3.2, 6.7, 16.7, 25.1, 28.3, 39.3, 61.5, 77.2, and 82.8 Hz. A random input excitation with zero mean and unit standard deviation is vertically applied at node 23. The dynamic responses of

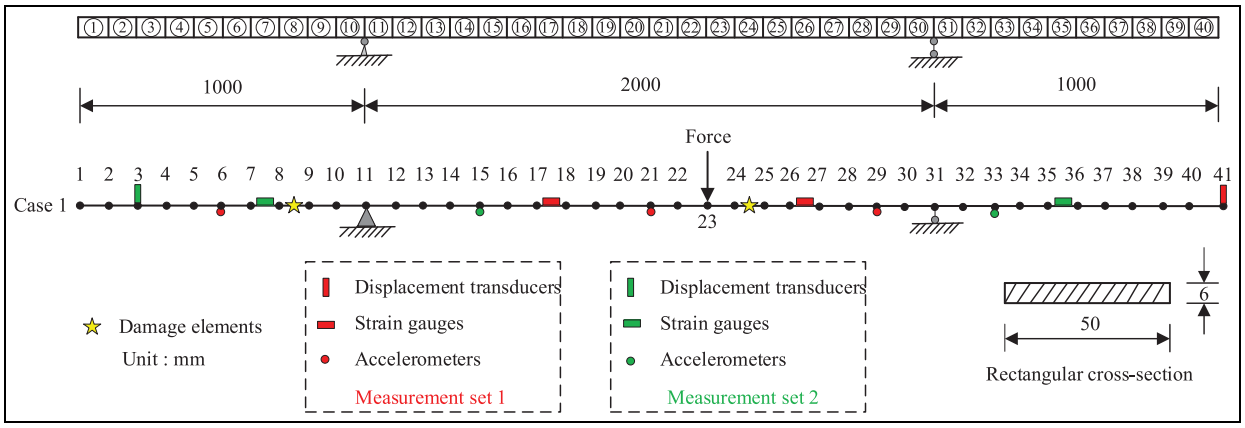

Figure 3. The numerical model of three-span beam structure.

the beam structure are recorded by multitype sensors, that is, displacement transducers, strain gauges, and accelerometers. It is noted that vertical nodal displacements and accelerations are measured by displacement transducers and accelerometers, while the flexural deformations are measured by strain gauges attached to the upper surface at the middle of selected elements.

As presented in Figure 3, in case 1, all sensors are divided into two different sets, that is, measurement set 1 and measurement set 2. The measurement set 1 consists of six heterogeneous measurements, including one displacement response (from node 41), two strain responses (from elements 17 and 26), and three acceleration responses (from nodes 6, 21 and 29). The measurement set 2 has five heterogeneous measurements including one displacement response (from node 3), two strain responses (from elements 7 and 35), and two acceleration responses (from nodes 15 and 33). The sampling frequency is set as 1000 Hz and sampling duration is defined as 1 s in this example. To investigate the adverse effect of measurement noise on the identification accuracy, white Gaussian noise is considered as follows:

$$Y_{mea} = Y_{clean} + N_1 \times N_{noise}\, RMS(Y_{clean}) \tag{40}$$

where Y_{clean} and Y_{mea} stand for the clean and noise-polluted signals; N_1 represents noise level; N_{noise} implies the standard normal distribution vector with zero mean and unit standard deviation; $RMS(Y_{clean})$ denotes the root mean square of clean response Y_{clean}. Herein, three levels of noise, that is, 0%, 5% and 10% are considered.

Results of response reconstruction

In order to verify the performance of the heterogeneous response reconstruction with Bayesian inference regularization technique, the intact finite element model is first regarded as the known. The responses from measurement set 1 are utilized to reconstruct the unmeasured input force and the responses of measurement set 2. The relative error (RE) and Pearson correlation coefficient (PCC) are used to evaluate the deviation and linear correlation degree between the measured and reconstructed measurements as follows:

$$RE = \frac{\|Y_{rec} - Y_{mea}\|_2}{\|Y_{mea}\|_2} \times 100\% \tag{41}$$

$$PCC(Y_{mea}, Y_{rec}) = \frac{Cov(Y_{mea}, Y_{rec})}{\sigma_{Y_{mea}} \sigma_{Y_{rec}}} \tag{42}$$

where Cov stands for covariance; σ means standard deviation.

Figures 4 and 5 present the results of reconstructed strain responses at element 7 and reconstructed acceleration responses at node 33, respectively. It is observed that the reconstructed and real responses are almost overlapping. In Figures 4(b) and 5(b), the discrepancy amplitudes are 2.5×10^{-16} and 3×10^{-10} for noise free case, indicating the good accuracy of response reconstruction. When contaminated with 10% noise, the PCC between the measured and reconstructed responses of set 2, as listed in Table 1, are 0.9945, 0.9941, 0.9949, 0.9938, and 0.9938, which also demonstrates that a good accuracy of structural response reconstruction is achieved. In addition, the unmeasured input force is reconstructed and presented in Figure 6. The reconstructed force matches well with the actual value without noise in both time domain and frequency domain. Obvious discrepancies between the reconstructed forces and actual value are observed in time domain with 10% noise, while compared to the natural frequencies of beam structure, the frequency component of the identified force within the range of 0–100 Hz matches well with the actual value even under 10% noise, which explains the effectiveness of the proposed method in force reconstruction.

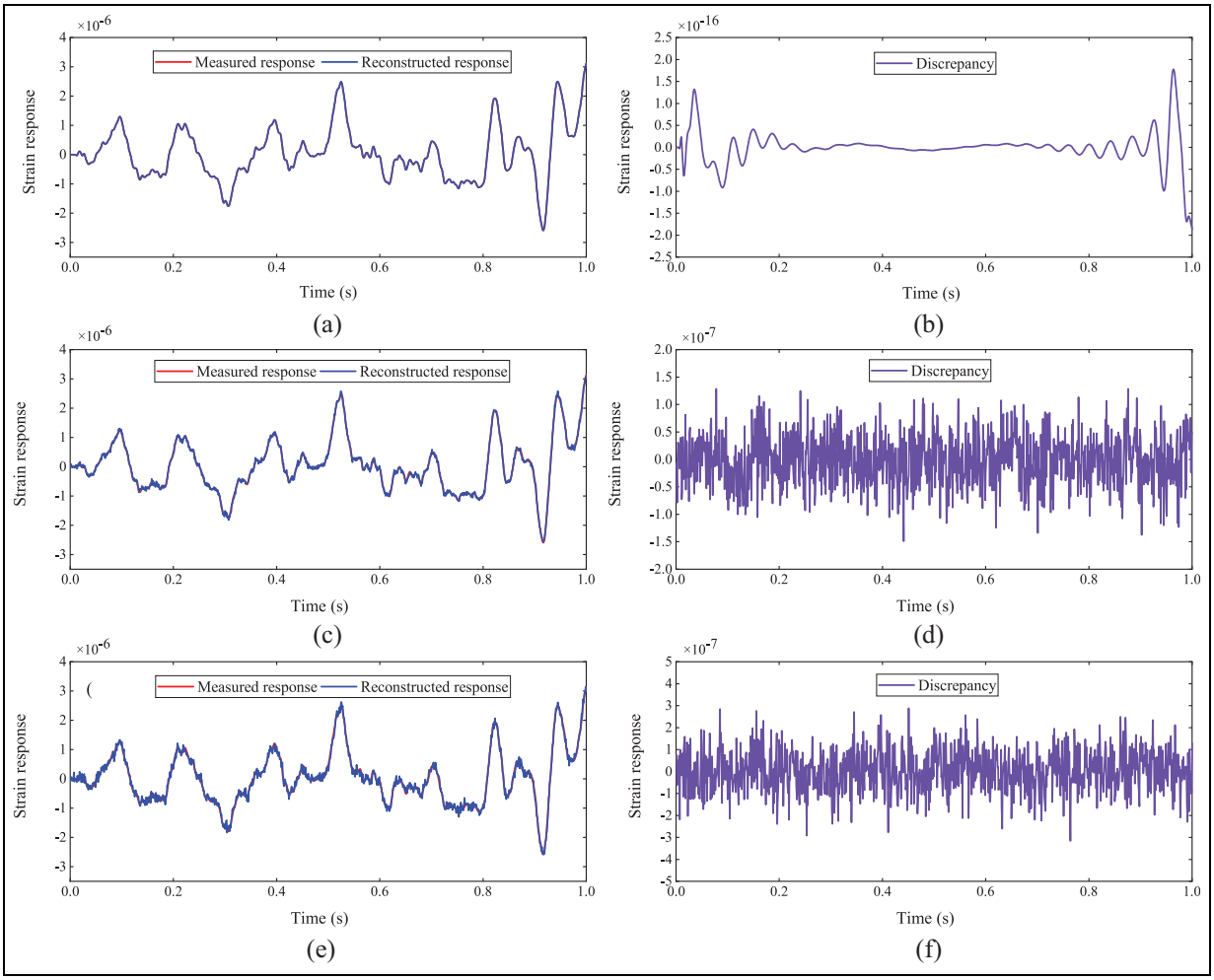

Figure 4. Measured and reconstructed strain responses at element 7: (a) comparison without noise, (b) discrepancy without noise, (c) comparison with 5% noise, (d) discrepancy with 5% noise, (e) comparison with 10% noise, and (f) discrepancy with 10% noise.

Damage identification with QHEA

In the proposed output-only identification strategy, both external excitation and actual damages of three-span beam structure are unknown. In case 1, it is assumed that there are 20% and 30% stiffness reductions at the 8th and 24th elements, namely, $\alpha_8 = 0.2$, $\alpha_{24} = 0.3$. For the parameters of the proposed QHEA, population size and maximum iteration number are set as 100 and 400, respectively. Figure 7 shows the identified results with the proposed QHEA under three levels of noise. Table 2 gives the calculated mean errors and maximum errors. It can be found that pleasant identification results are achieved with mean errors of 0.15%, 0.36%, 0.81%, as well as the maximum errors of 1.78%, 3.22%, 4.77% corresponding to the cases of noise free, 5% noise, and 10% noise, respectively. Besides, the effect of modeling errors on the identification results is investigated. To consider the modeling errors in numerical structure, 1% uncertainty with Gaussian distributions is added into the stiffness parameters for all elements.[47] Figure 8 presents the identified damage extents with modeling errors. Obviously, damage locations and extents of elements 8 and 24 are successfully detected. By Table 2, 1.14% mean error and 5.02% maximum error are identified for 10% noise case, which implies the proposed method can accurately detect structural damages even if taking the measurement noise and modeling errors into account.

Taking the evolutionary process of identified damaged extents under 5% noise for example, Figure 9 presents the identified damage extents with iteration by the proposed QHEA. Around 100 iterations are needed to approach the exact values. After 400 iterations, the identified damage extents are $\alpha_8 = 0.1699$ and $\alpha_{24} = 0.3207$. The estimated damage indexes agree well with the actual values.

Comparison with other algorithms

In this section, to show the superiority of QHEA, other three heuristic algorithms including modified

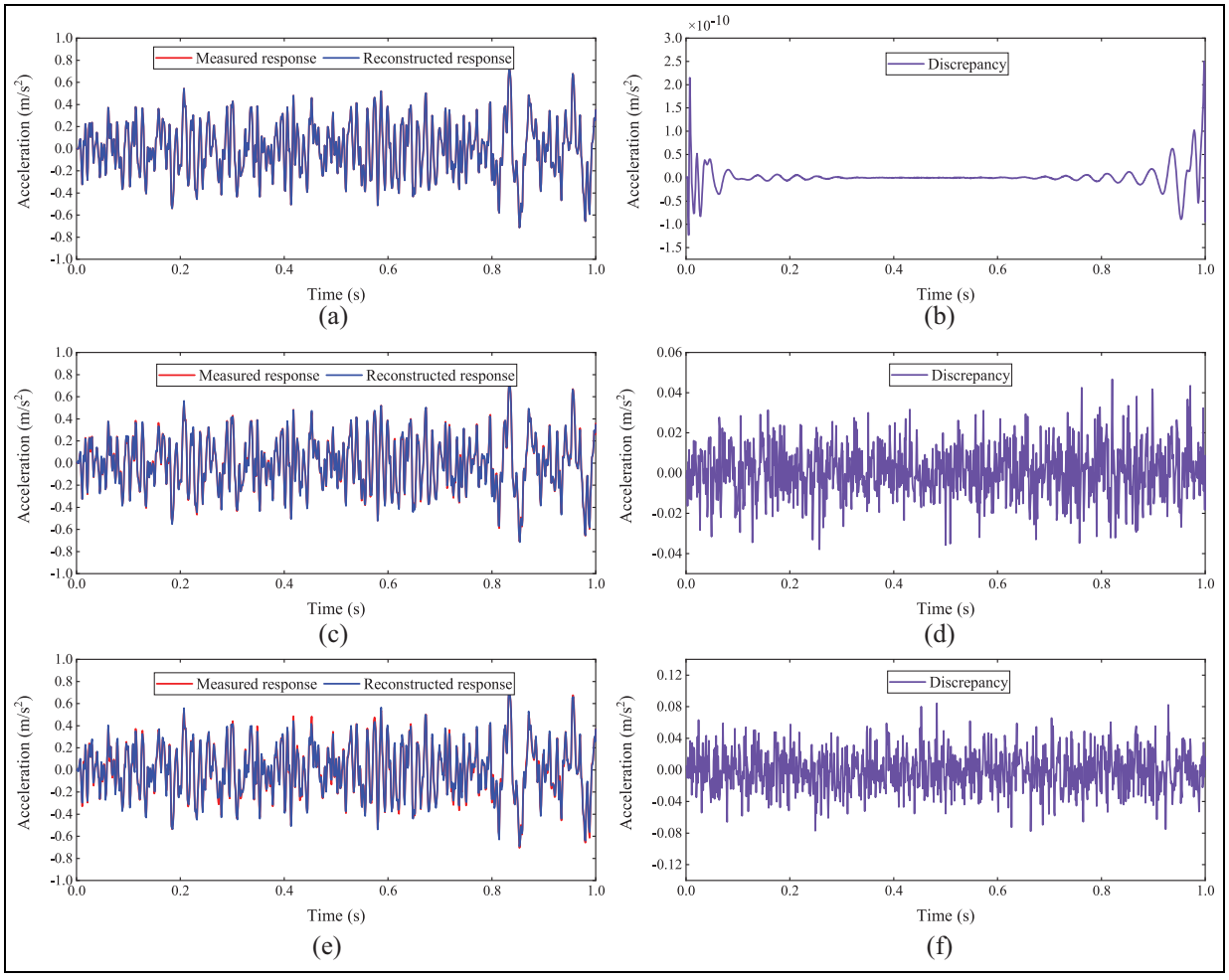

Figure 5. Measured and reconstructed acceleration responses at node 33: (a) comparison without noise, (b) discrepancy without noise, (c) comparison with 5% noise, (d) discrepancy with 5% noise, (e) comparison with 10% noise, and (f) discrepancy with 10% noise.

Table 1. RE and PCC of measurement set 2.

Type of reconstruction	0% noise		5% noise		10% noise	
	RE	PCC	RE	PCC	RE	PCC
Displacement response at node 3	8.17e-10	1.00	4.93	0.9988	10.47	0.9945
Strain response at element 7	4.13e-09	1.00	5.26	0.9986	10.83	0.9941
Strain response at element 35	6.34e-09	1.00	5.29	0.9986	10.04	0.9949
Acceleration response at node 15	2.91e-08	1.00	5.61	0.9984	11.15	0.9938
Acceleration response at node 33	1.07e-08	1.00	5.46	0.9985	11.17	0.9938

RE: relative error; PCC: Pearson correlation coefficient.

differential evolution algorithm (MDE),[48] Jaya algorithm, improved Jaya algorithm (I-Jaya)[31] are employed to estimate a new damage case, and their results are compared with that acquired by the proposed QHEA. The common parameter settings of MDE, Jaya, I-Jaya, QHEA, population size $NP = 100$, maximum iterations $Max\_Iter = 400$, tolerance $Tol = 5 \times 10^{-2}$, total evaluations = 40,000 are used. As for the algorithm-specific parameters, mutation rate and threshold value are 0.4 and 0.1 for MDE, respectively. Mutation rate, crossover rate, and discount factor are set as 0.8, 0.9, 0.8 for QHEA.

In the second damage case, it is assumed that there are 20%, 10%, 10%, 20% stiffness reductions at the 8th, 15th, 24th, and 32th elements, namely, $\alpha_8 = 0.2$, $\alpha_{15} = 0.1$, $\alpha_{24} = 0.1$, $\alpha_{32} = 0.2$. As presented in Figure 10,

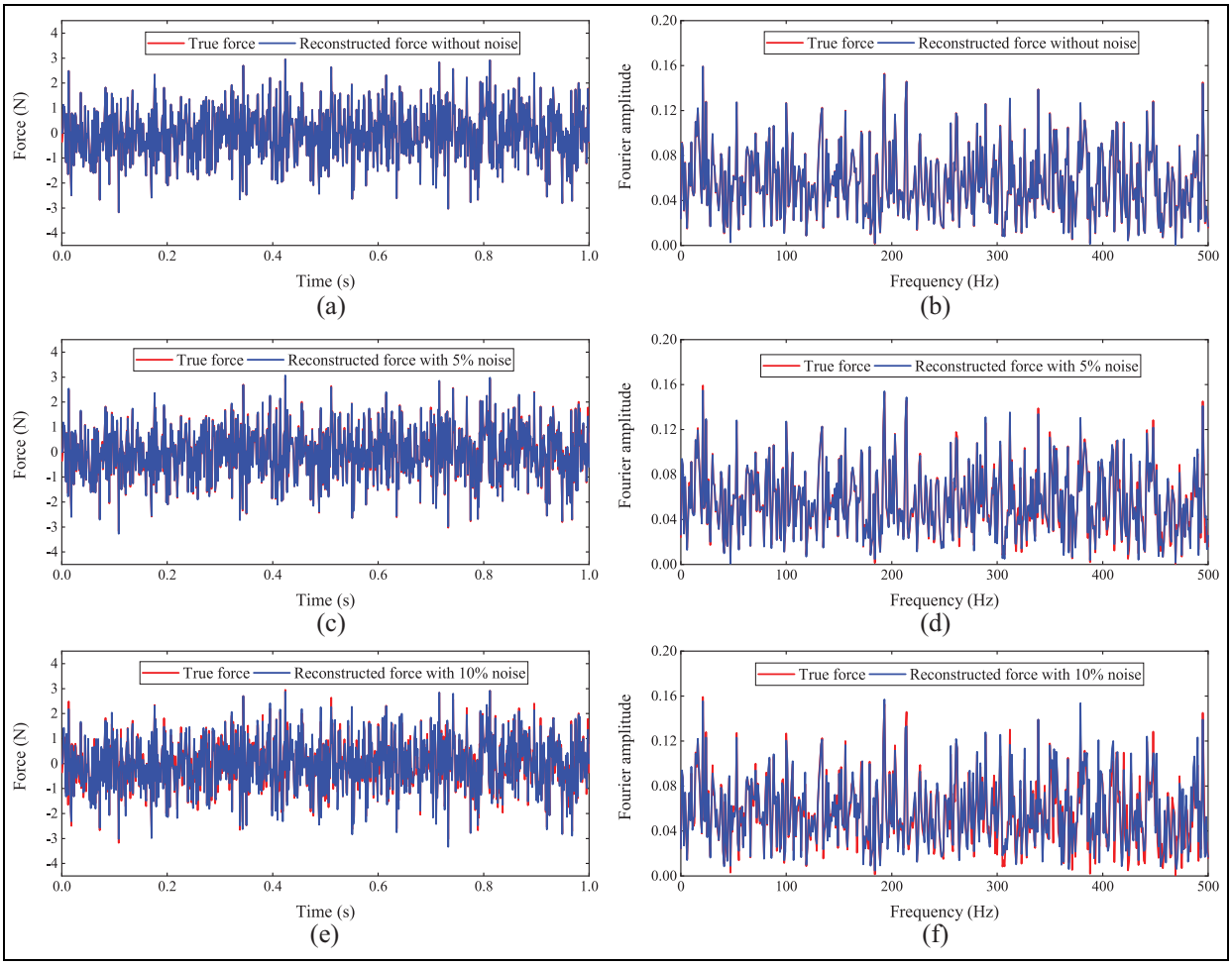

Figure 6. Comparison of the reconstructed force with actual value: (a) time history without noise, (b) frequency spectrum without noise, (c) time history with 5% noise, (d) frequency spectrum with 5% noise, (e) time history with 10% noise, and (f) frequency spectrum with 10% noise.

case 2 consists of 11 sensors installed on the structure with the same placement in Zhang and Xu,[36] and they can be divided into two different sets, that is, measurement set 1 and measurement set 2. The measurement set 1 has five heterogeneous measurements, including one displacement response (from node 41), two strain responses (from elements 11 and 31), and two acceleration responses (from nodes 1 and 26). The measurement set 2 contains six heterogeneous measurements, including one displacement response (from node 1), three strain responses (from elements 6, 21 and 35), two acceleration responses (from nodes 16 and 41).

Figure 11 shows the evolutionary process of objective function values based on MDE, Jaya, I-Jaya, QHEA for noise-free case. It is easily observed that the proposed QHEA is able to achieve faster convergence speed, and only 312 iterations are needed to meet convergence criteria. The objective function values acquired by MDE, Jaya, I-Jaya, QHEA are 0.4971, 0.1711, 0.0167, and 0.0014, respectively. The smallest value of QHEA demonstrates it can achieve the best identification results. Figure 12 presents the final identification results using MDE, Jaya, I-Jaya, QHEA, and REs of damage extents are listed in Table 3. It is clearly noticed that several large false identifications are obtained by MDE at elements 1, 3, 33, 39, 40, and the maximum RE are 82.64% for α_8. Similar to MDE, Jaya algorithm fails in identifying damage locations and extents accurately. Compared with MDE and Jaya, less errors are obtained by I-Jaya algorithm, but it still has some difficulties in estimating the damage extents at elements 8 and 24. In contrast, as illustrated in Figure 12 and Table 3, the proposed QHEA provides the most satisfactory identification results with only 3.21% maximum RE for identified damage extents. These results imply that the balance between global exploration and local exploitation of the proposed QHEA is well realized by adaptively selecting the best action from strategy pool.

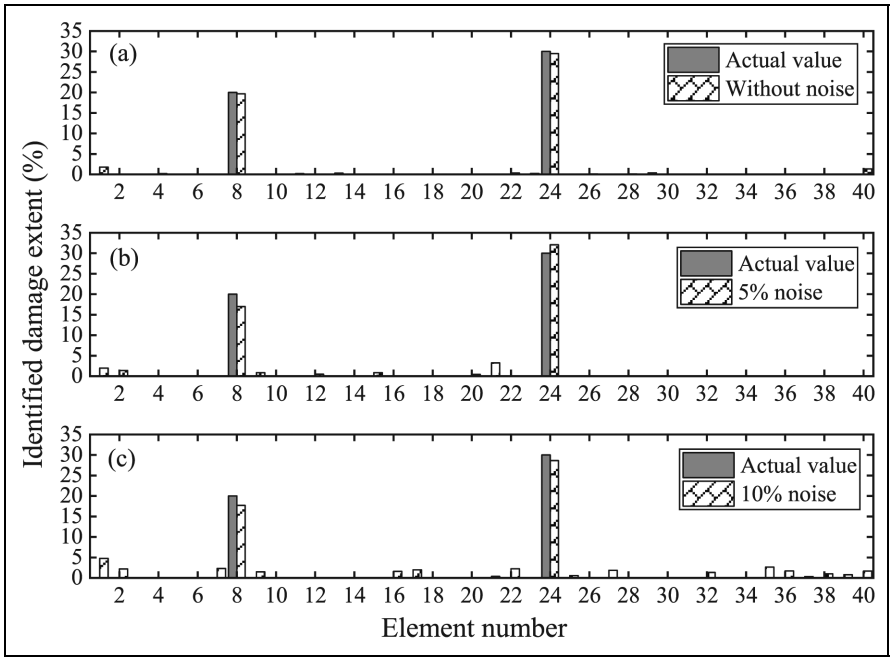

Figure 7. Identified damage results without modeling errors for case 1: (a) 0% noise, (b) 5% noise, and (c) 10% noise.

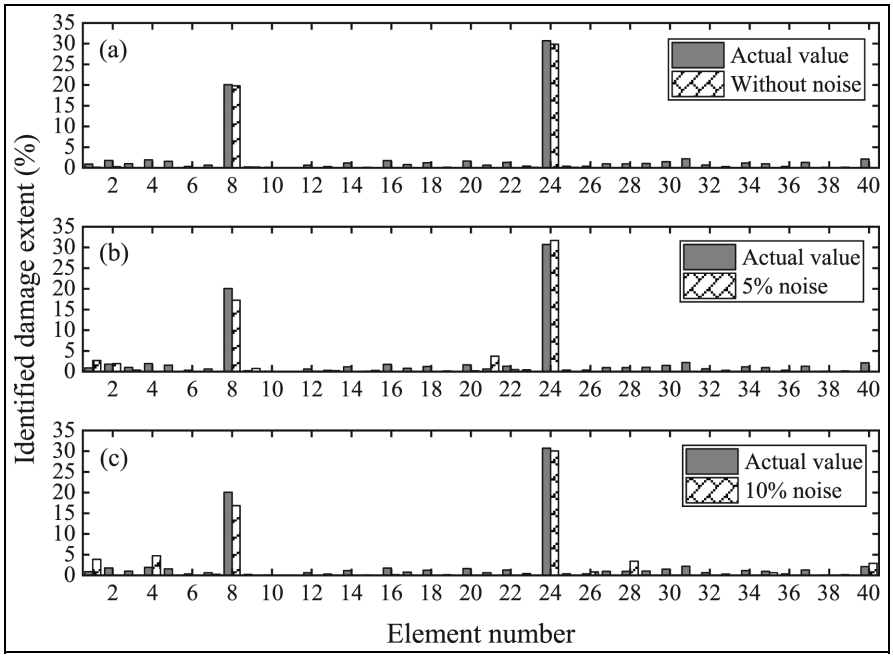

Figure 8. Identified results considering modeling errors for case 1: (a) 0% noise, (b) 5% noise, and (c) 10% noise.

Table 2. Identified results using QHEA for case 1 with and without initial modeling errors (%).

Cases	0% noise		5% noise		10% noise	
	Mean error	Max error	Mean error	Max error	Mean error	Max error
Without modeling error	0.15	1.78	0.36	3.22	0.81	4.77
With modeling error	0.86	2.21	1.09	3.71	1.14	5.02

QHEA: Q-learning hybrid evolutionary algorithm.

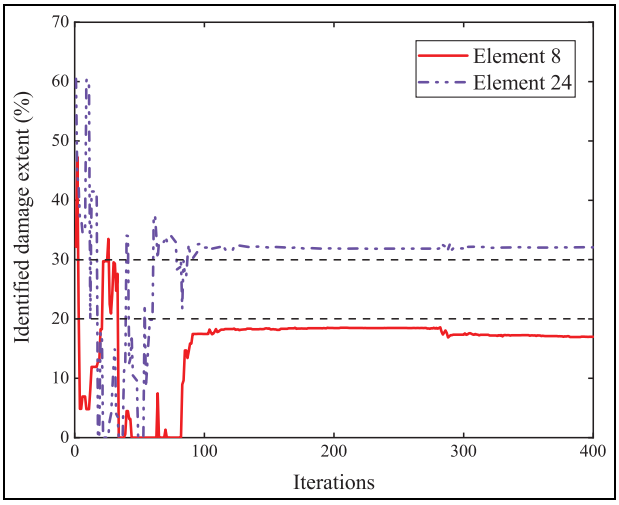

Figure 9. The evolutionary process of identified damaged extents for three-span beam structure (5% noise).

Experimental studies

Description of structural model

Experimental studies on a five-floor steel frame model in the laboratory are carried out to further validate the effectiveness of the proposed output-only strategy for structural damage identification. Figure 13 depicts the experimental setup and geometric dimensions of laboratory model. The height, length, and width of the frame structure are 1750, 300, and 400 mm, respectively. In each floor, the dimensions of story slab are $300 \times 400 \times 15$ mm, and there are four identical columns with the cross-section of 40×4 mm. The finite element model of the steel frame can be simplified as a 5-DOF shear-type system in consideration of the comparatively strong floors and weak columns. The mass density and initial elastic modulus of steel material are 7850 kg/m^3 and 2.06×10^{11} N/m^2, respectively. A vibration exciter (Modal Shop 2100E11) is anchored on counterforce wall to provide sinewave input excitation at the top floor of frame structure. A power amplifier is employed to generate sufficient power to actuate the vibration exciter. In order to directly measure external input excitation, as shown in Figure 14(a), a force sensor (PCB208C02) is installed between the shaker and the frame model. By Figures 13 and 14(b), it is also observed that five model 991C accelerometers and five displacement transducers are used to record the horizontal acceleration and displacement responses of each floor with the Quantum X data acquisition system. According to the theory of response reconstruction technique with multitype sensors, heterogeneous measurements are divided into two sets. The measurement set 1 consists of displacement and acceleration responses of the first, third, fifth floors, and the measurement set 2 contains displacement and acceleration responses of the other floors. A 20 s vibration data with sampling frequency of 50 Hz is recorded for initial model updating and damage identification.

Based on the estimation of the geometric information and material property, the lumped masses of five stories including accelerometer are known, that is, $M_1 = 24.99$ kg, $M_2 = 24.94$ kg, $M_3 = 24.93$ kg, $M_4 = 24.75$ kg, $M_5 = 24.80$ kg, respectively. As listed in Table 4, the measured natural frequencies are obtained by the peak-picking method from the vibration measurements, and their values are 1.998, 5.988, 8.990, 11.962, 14.988 Hz. The analytical frequencies using the finite element method in intact state are 2.022, 5.856, 9.274, 11.915, 13.584 Hz. More than 9.3% maximum RE indicates that there are large modeling errors in the established initial finite element model. To calibrate the finite element model, initial model updating is conducted by adjusting stiffness parameters with the proposed QHEA. Regarding the parameter settings of QHEA,

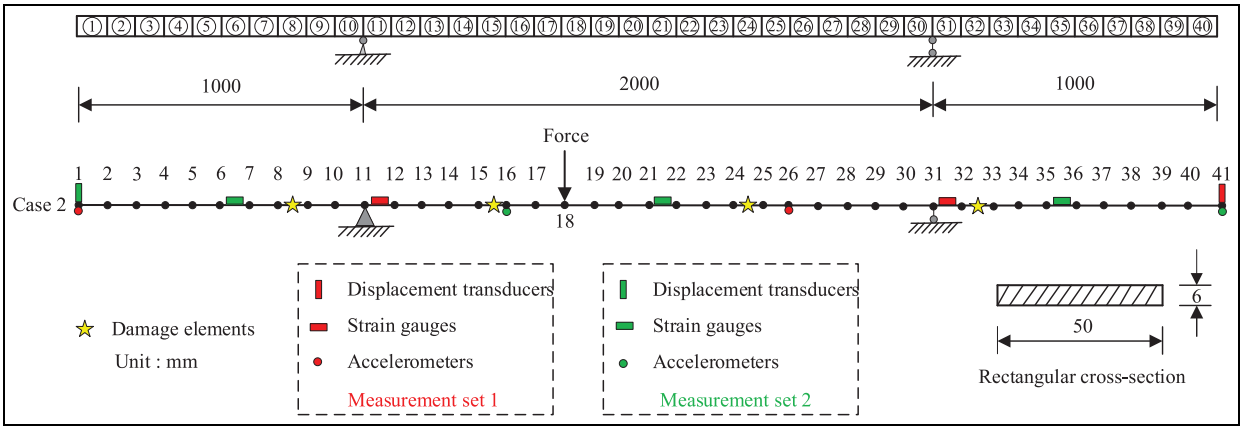

Figure 10. The placement of multitype sensors in case 2.

population size and maximum number of iterations are set as 40 and 200. It is observed from Table 4 that the discrepancies of model frequencies between the numerical model after updating and the experimental model are significantly decreased with less than 2% maximum RE. Thus, the updated model matches the experimental model well, so it can be regarded as baseline model in the subsequent structural damage identification.

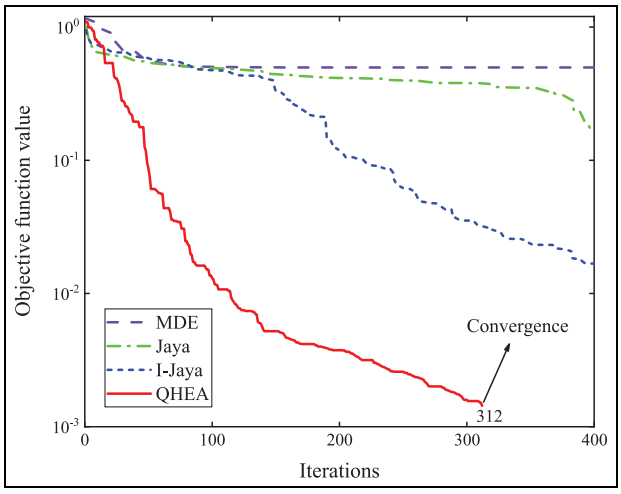

Figure 11. The evolutionary process of objective function values for MDE, Jaya, I-Jaya, and QHEA.
MDE: modified differential evolution algorithm; QHEA: Q-learning hybrid evolutionary algorithm; I-Jaya: improved Jaya algorithm.

To check the accuracy of response reconstruction with experimental data, taking the responses in the first second, for example, Figure 15 shows the measured and reconstructed acceleration responses of the second floor and the fourth floor. The reconstructed responses agree well with the measured ones with the REs of 4.74%% and 3.74%, respectively. In addition, the mean squared error (MSE), root mean square error (RMSE), and mean absolute error (MAE) are also calculated to evaluate the accuracy of response reconstruction. MSE are 0.0037 and 0.0036 for the second floor and fourth floor, RMSE are 0.0609 and 0.0603 for the second floor and fourth floor, MAE are 0.0497 and 0.0485 for the second floor and fourth floor.

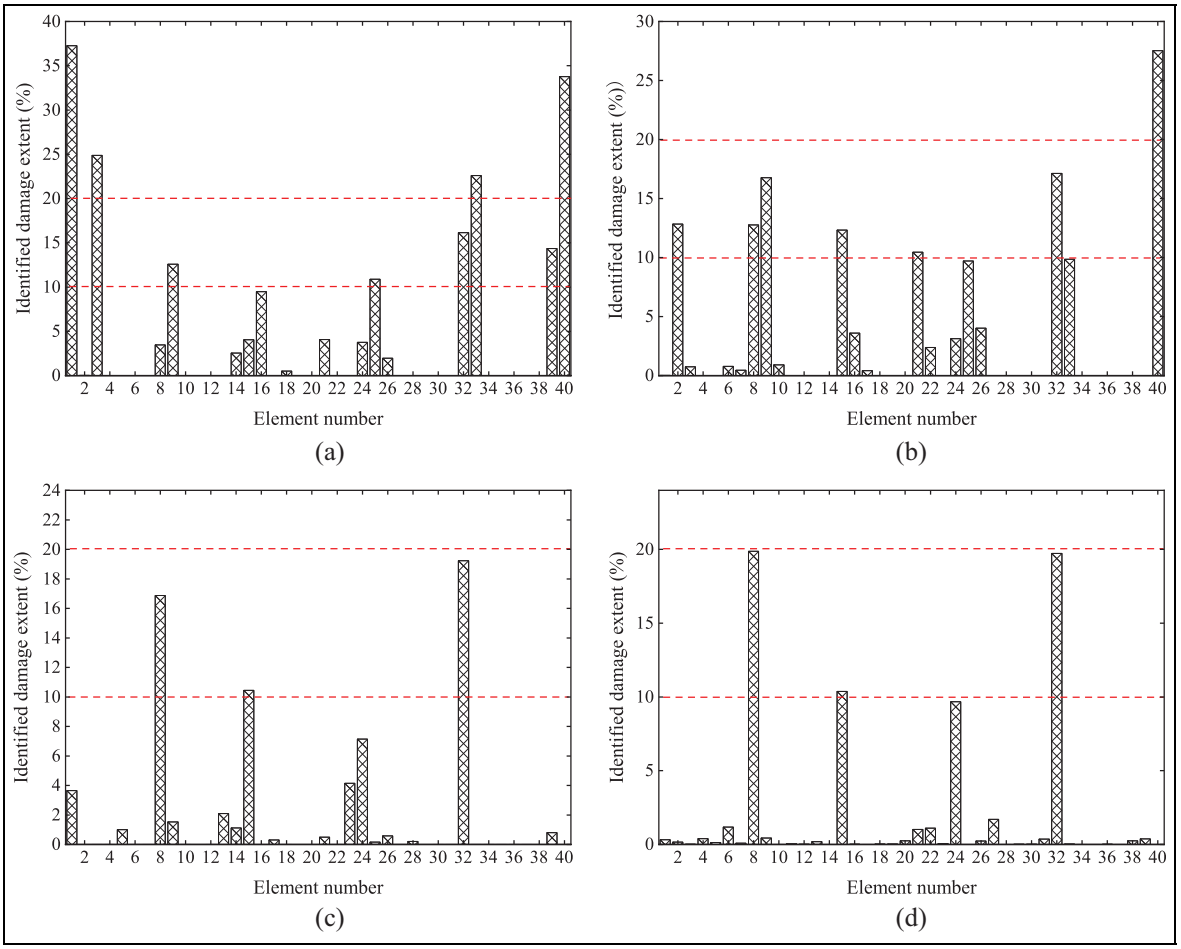

Figure 12. Identified damage results in case 2 using: (a) MDE, (b) Jaya, (c) I-Jaya, and (d) QHEA.
MDE: modified differential evolution algorithm; QHEA: Q-learning hybrid evolutionary algorithm; I-Jaya: improved Jaya algorithm.

Table 3. Identified damage extents and their relative errors using MDE, Jaya, I-Jaya, and QHEA.

Damage location	True value	MDE Identified	Error (%)	Jaya Identified	Error (%)	I-Jaya Identified	Error (%)	QHEA Identified	Error (%)
α_8	0.2	0.0347	82.64	0.1277	36.17	0.1687	15.63	0.1987	0.64
α_{15}	0.1	0.0405	59.49	0.1233	23.33	0.1045	4.47	0.1037	3.65
α_{24}	0.1	0.0377	62.33	0.0312	68.79	0.0714	28.60	0.0968	3.21
α_{32}	0.2	0.1613	19.33	0.1712	14.39	0.1923	3.85	0.1972	1.39

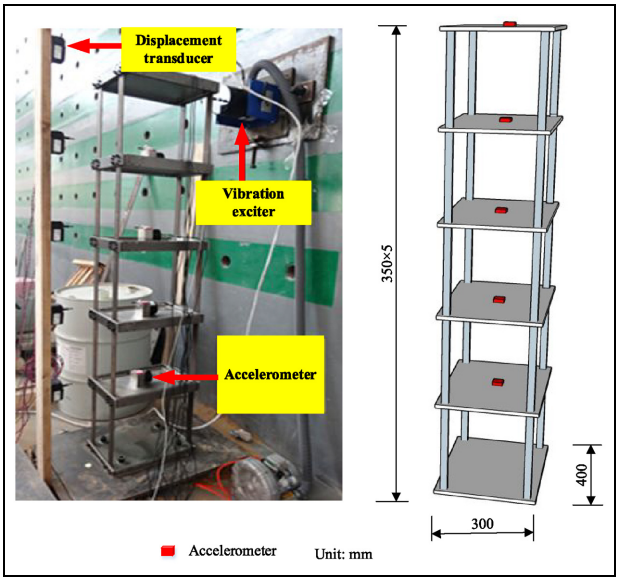

Figure 13. The experimental setup of five-floor steel frame structure.

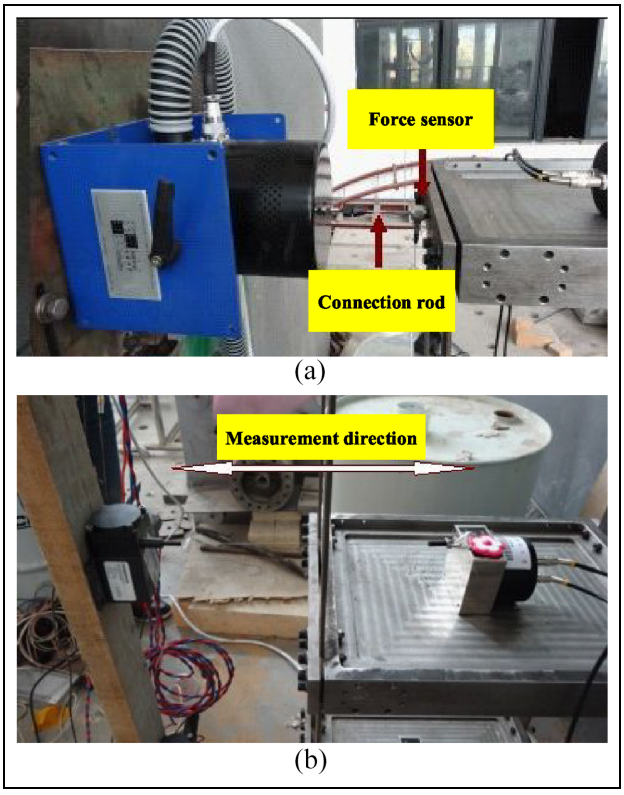

Figure 14. Experimental details: (a) applying external load (b) measurement direction.

Identification of two damages scenarios

In order to test the performance of the proposed method in detecting, localizing, and quantifying structural damages, artificial damages are introduced into the steel frame structure by reducing the cross-section of columns. Two damage scenarios are considered, and four tests are implemented in each damage scenario. All columns in the fifth floor are replaced from original width of 40 mm to a smaller width of 36 mm, denoted as scenario 1, which results in 10% stiffness reduction for element 5. In the same way, all columns in the fourth floor are replaced from original 40 mm to more thinner 32 mm, named as scenario 2, which leads to 20% equivalent stiffness reduction for element 4. Herein, mass alteration can be directly neglected owing to less than 2% slight reductions of mass in these two damage scenarios, rendering it hard to be successfully detected.

Table 4. Measured and analytical natural frequencies of frame structure before and after updating.

Mode	Measured	Before updating		After updating	
	(Hz)	Analytical (Hz)	Relative error (%)	Analytical (Hz)	Relative error (%)
1	1.998	2.033	1.752	1.992	0.300
2	5.988	5.874	1.904	5.965	0.384
3	8.990	9.246	2.848	9.041	0.567
4	11.962	11.904	0.485	12.010	0.401
5	14.988	13.594	9.301	14.689	1.995

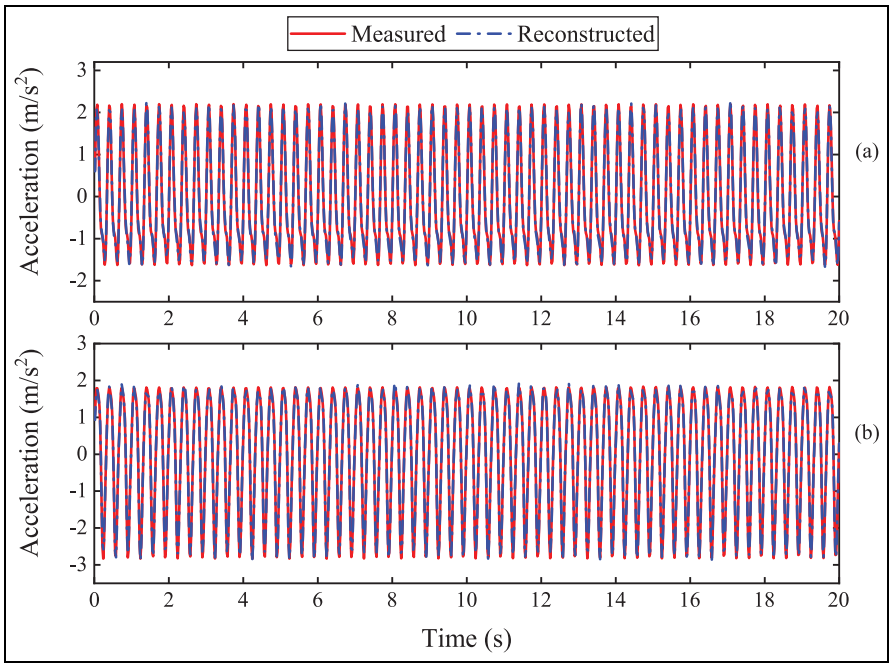

Figure 15. Comparison of measured and reconstructed values: (a) acceleration of the second floor and (b) acceleration of the fourth floor.

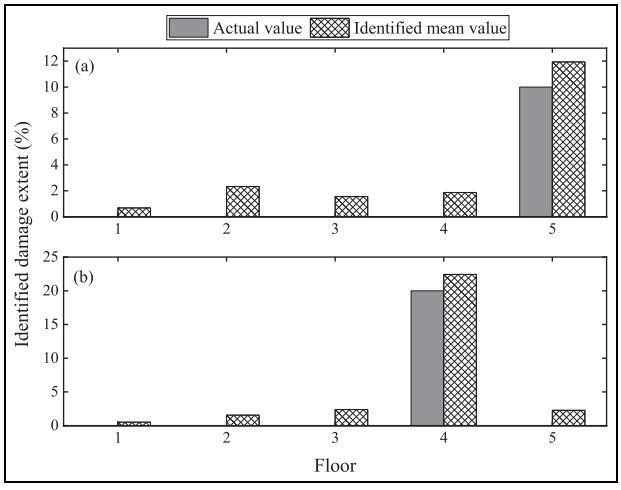

Figure 16. Identified damage results with proposed output-only method: (a) scenario 1 and (b) scenario 2.

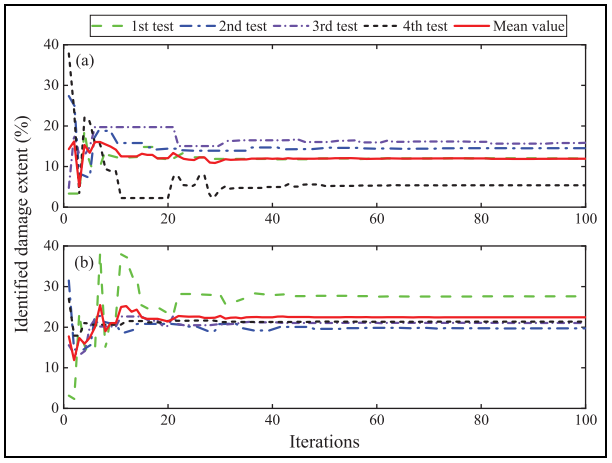

Figure 17. The convergence process of the identified damage extents: (a) scenario 1 and (b) scenario 2.

The measurement set 1 is used to reconstruct the responses of the measurement set 2. Structural damages are identified by minimizing the difference between the measured and reconstructed responses in the second set. In consideration of the superior performance than MDE, Jaya, I-Jaya in section "Comparison with other algorithms," only the proposed QHEA is utilized as search tool, and its parameter settings are defined as the same values in the previous initial model updating. Figure 16 provides the mean values of identified damage results for scenario 1 and scenario 2. In scenario 1, the identified damage extent in the fifth floor is 11.94%. For scenario 2, the identified damage extent in the fourth floor is 22.43%. Both damage locations and severities can be well identified. In addition. Figure 17 presents the convergence process of the identified damage extents. It is clearly observed that after around 40 iterations, the identified mean values converge to the neighborhood of the actual damage extents. More reliable identification results are obtained if more tests are available. The

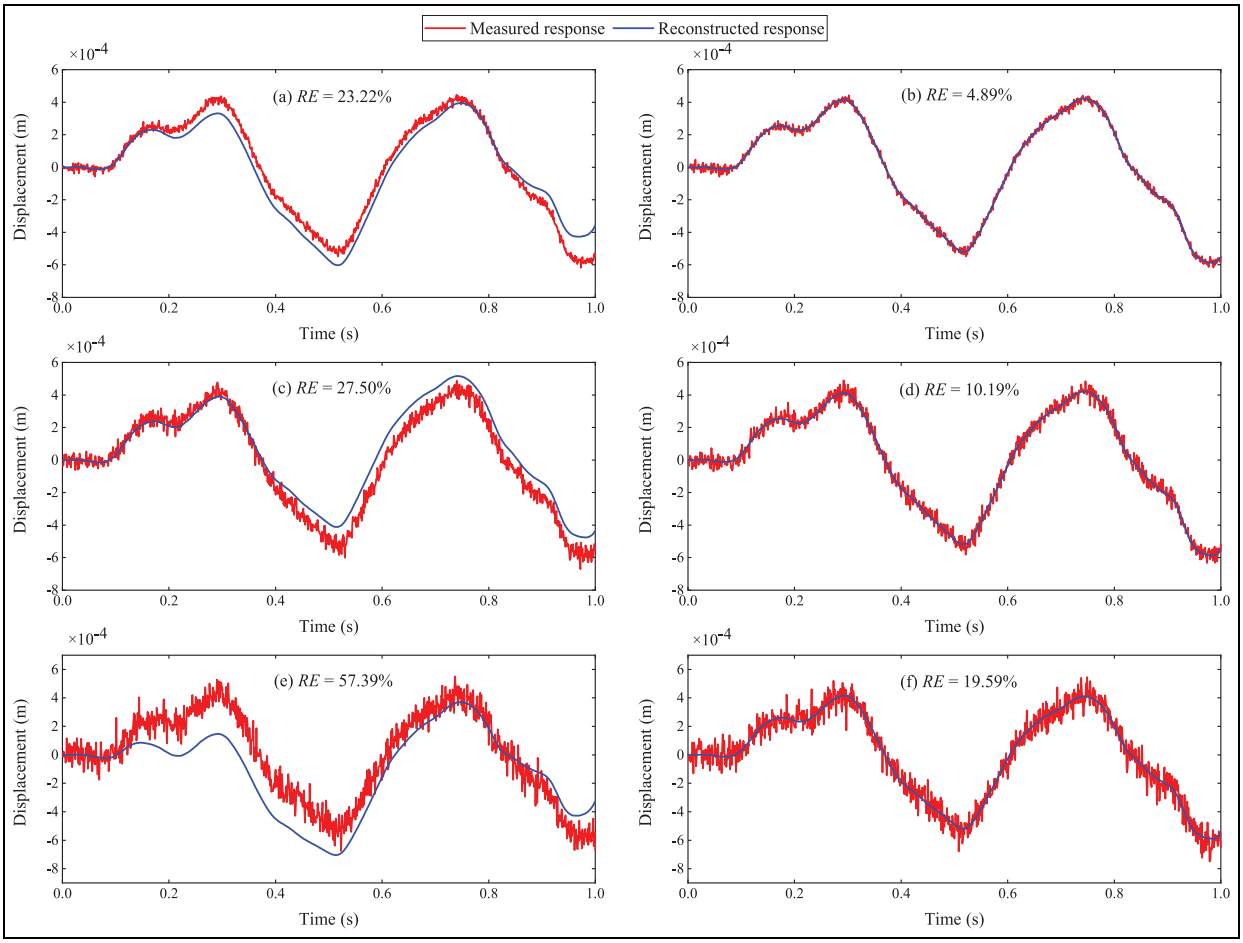

Figure 18. The reconstructed displacement response from node 1: (a) unscaled data with 5% noise, (b) rescaling data with 5% noise, (c) unscaled data with 10% noise, (d) rescaling data with 10% noise, (e) unscaled data with 20% noise, and (f) rescaling data with 20% noise.

experimental study demonstrates the proposed method can be successfully applied into output-only structural damage identification.

Discussions

The effect of data rescaling. In practice, the magnitudes of heterogeneous measurements, such as displacements, strains, and accelerations are very different. Under such circumstances, data rescaling is introduced in Equations (27)–(29). After rescaling the data, the magnitudes of the heterogeneous responses become a similar order. In order to investigate the effect of data rescaling on response reconstruction, the case 2 in section "Comparison with other algorithms" is employed as an example. The responses of measurement set 2 are reconstructed with unscaled data (rescaling coefficients $a_u = 1$, $a_\varepsilon = 1$, $a_{\ddot{u}} = 1$) and rescaled data of measurement set 1, respectively. Figure 18 shows the reconstructed displacement response from node 1 under 5%, 10% and 20% noise cases. RE is calculated to illustrate the accuracy of identified results. It is observed that obvious drifts are presented in the identified displacement response using unscaled data, and REs are 23.22%, 27.50%, and 57.39% with 5%, 10%, and 20% noises. In contrast, the reconstructed responses match the measured response well using rescaled data, and smaller REs are noticed. Therefore, it can be concluded that data rescaling is indispensable for heterogeneous data fusion.

The effect of data fusion

To demonstrate the superiority of heterogeneous data fusion for structural damage identification, other three conditions using only one type of response, that is, displacement, strain, or acceleration, are considered. In case 3, assuming there are 5%, 10%, 10%, 20% stiffness reductions at the 8th, 15th, 24th, and 32th

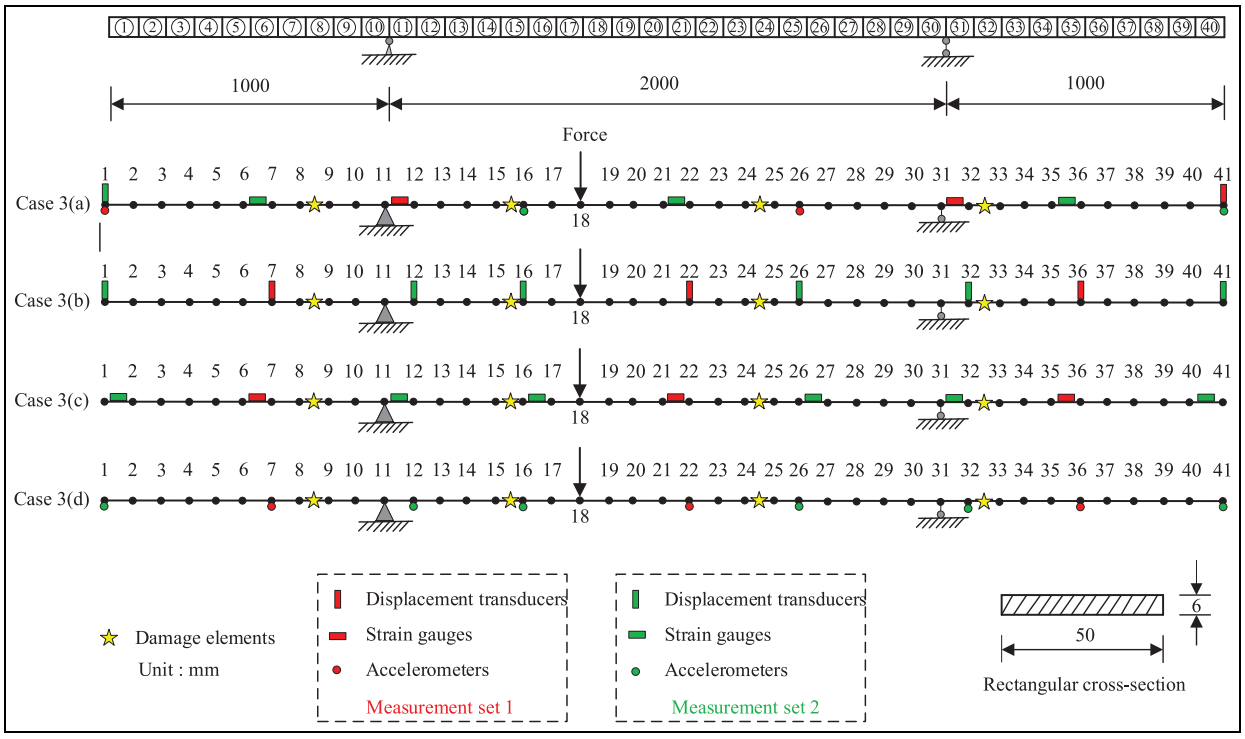

Figure 19. Four sensor placement configurations of three-span beam structure for case 3.

elements, namely, $\alpha_8 = 0.05$, $\alpha_{15} = 0.1$, $\alpha_{24} = 0.1$, $\alpha_{32} = 0.2$. As displayed in Figure 19, same sensor placement configuration of case 3(a) is used as case 2. In case 3(b), nine displacement transducers are installed on equivalent locations (nodes 1, 7, 12, 16, 22, 26, 32, 36, 41). In case 3(c), nine strain gauges are arranged on equivalent locations (elements 1, 6, 11, 16, 21, 26, 31, 35, 40). In case 3(d), nine accelerometers are mounted on equivalent locations (nodes 1, 7, 12, 16, 22, 26, 32, 36, 41). The responses belonging to measurement set 1 and measurement set 2 are represented by red and green colors, respectively.

The proposed QHEA is utilized as search tool, and its population size and maximum iteration number are set as 100 and 400. The results using four sensor placement configurations are shown in Figures 20 to 22, corresponding to 0% noise case, 5% noise case, and 10% noise case, respectively. It is noted that both damage locations and severities are not successfully identified with only displacement or strain responses. Strain responses are generally sensitive to small damages but considerable strain gauges need to be installed to obtain the point-to-point local damage information. Instead, accelerometers can detect the structural health state at a global level, while the small or minor damages may not be identified. Just as presented in Figure 20(d), the 5% damage at element 8 is identified as intact using acceleration responses only. In the results of 5% and 10% noise cases, as listed in Table 5, the maximum errors for case 3(d) are 9.50% and 10.00%. For the case 3(a), the identification results using multitype sensors are satisfactory. When contaminated with 10% noise, the damage extents are still accurately identified and errors of other elements are acceptable, which implies the superiority of heterogeneous data fusion.

Conclusion

In this article, a novel output-only structural damage identification approach based on reinforcement-aided evolutionary algorithm and heterogeneous response reconstruction with Bayesian inference regularization is proposed. Multitype responses including displacements, strains, and accelerations are fused and rescaled for response reconstruction. Damage identification is transformed into minimizing the difference between the measured and reconstructed responses. In order to solve the optimization-based inverse problem, QHEA integrating Jaya algorithm, differential algorithm, and Q-learning algorithm is developed. To verify the effectiveness of the proposed method, numerical studies on a three-span beam structure and a series of experimental studies on a five-floor steel frame structure are

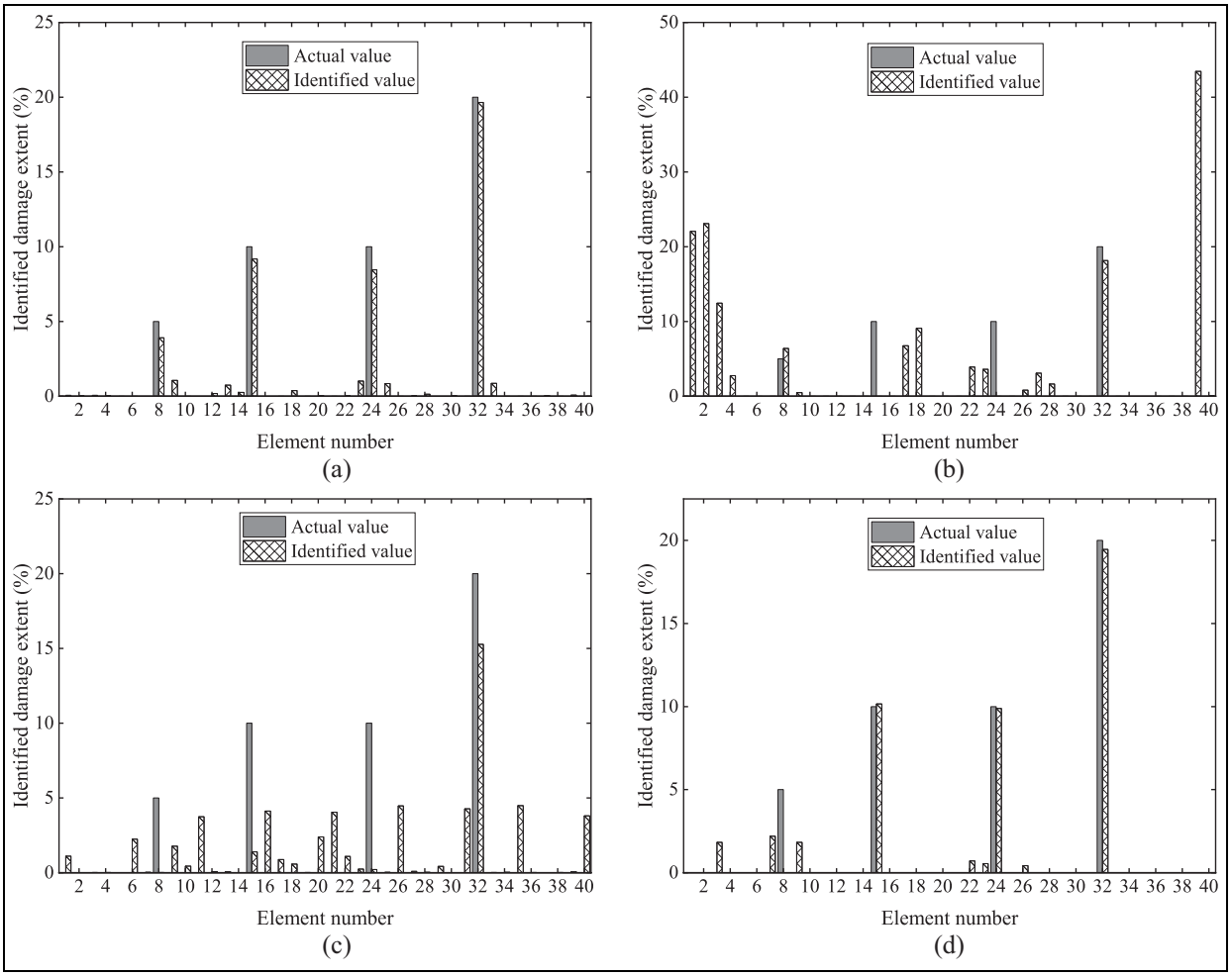

Figure 20. Damage results with different sensor placement configurations under 0% noise: (a) case 3(a), (b) case (3b), (c) case 3(c) and (d) case 3(d).

conducted. In addition, the effects of data rescaling and data fusion are discussed. Some interesting conclusions can be drawn as follows:

(1) The results of RE and PCC demonstrate a good accuracy of structural response reconstruction is achieved with the aid of Bayesian inference regularization, while obvious drifts are presented in the identified displacement response using unscaled data, so data rescaling is indispensable for heterogeneous data fusion.
(2) The proposed QHEA can accurately detect structural damages even if taking the measurement noise and modeling errors into account, and it can achieve faster convergence speed and more satisfactory identification results than MDE, Jaya, I-Jaya, since exploration and exploitation could be better balanced.
(3) Compared with one type of responses, more superior performance is obtained by using multi-type responses since heterogeneous data fusion can effectively combine the individual advantages of displacement, strain, acceleration measurements, which is more practical and suitable for the structural health monitoring of large-scale civil structures.
(4) By integrating reinforcement learning, heterogeneous response reconstruction, and Bayesian inference regularization, the proposed approach offers a promising direction for enhancing the accuracy, reliability, and efficiency of output-only damage identification methods.

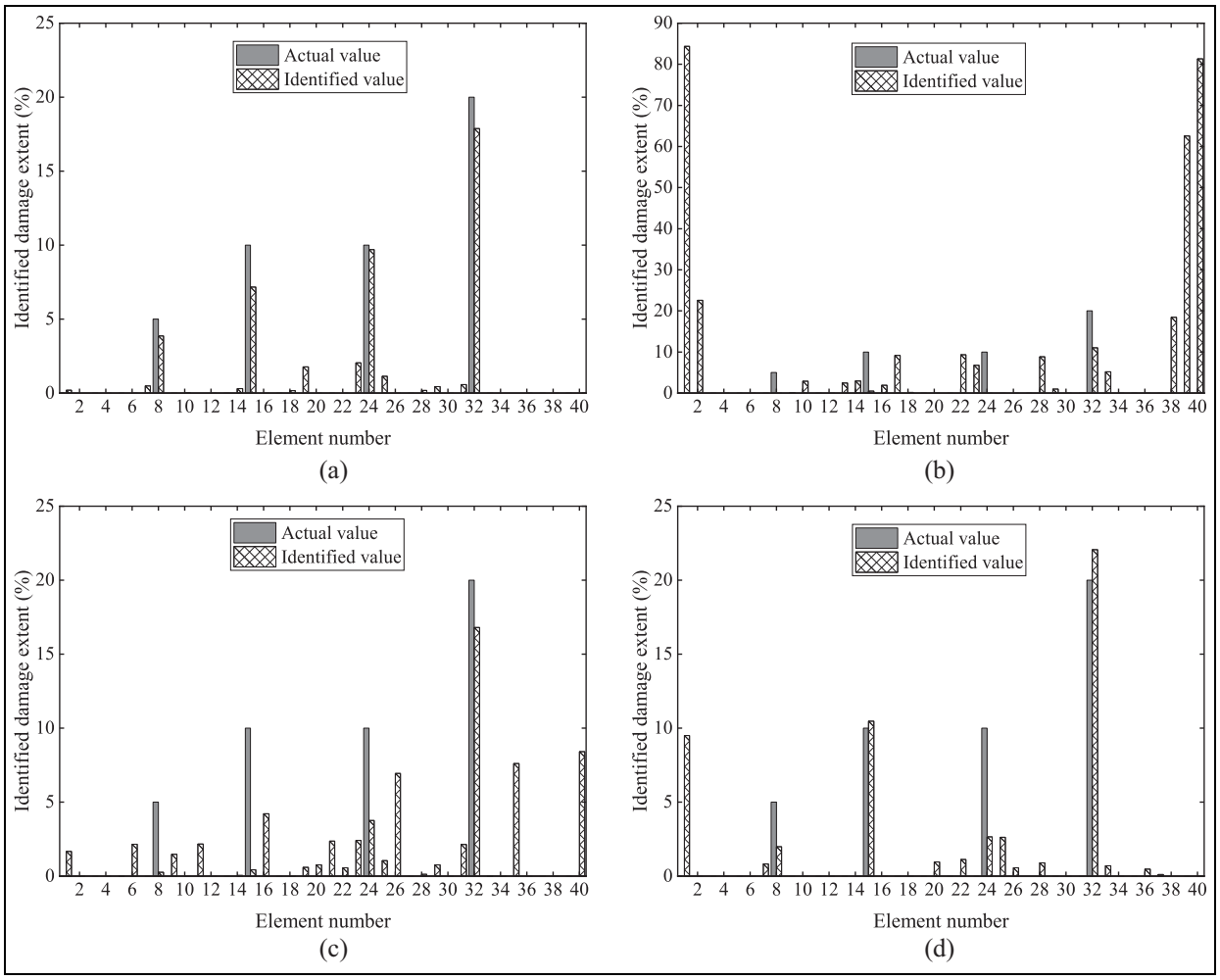

Figure 21. Damage results with different sensor placement configurations under 5% noise: (a) case 3(a), (b) case (3b), (c) case 3(c) and (d) case 3(d).

Table 5. Identified errors with different sensor placement configurations (%).

Cases	0% noise		5% noise		10% noise	
	Mean error	Max error	Mean error	Max error	Mean error	Max error
Case 3(a)	0.24	1.55	0.34	2.83	0.69	4.60
Case 3(b)	3.91	43.45	8.84	84.41	11.82	84.62
Case 3(c)	1.72	9.79	1.73	9.58	2.05	9.98
Case 3(d)	0.33	5.00	0.77	9.50	1.24	10.00

The limitation of this study is the optimal sensor placement configuration for heterogenous sensors is not considered. The proposed method requires that the number of sensors in the measurement set 1 exceeds the number of unknown external excitations on the structure, which is difficult to meet under some conditions. Besides, contact dense sensor networks need to be installed on the large-scale and complex civil structures owing to their pointwise measurement characteristic, which would be high-cost and time-consuming. Displacement measurements are crucial to evaluate the health state of target structure but tend to be difficult to measure directly. Noncontact vision-based techniques have emerged as promising tools for remote measurement of displacement responses. Hence, data fusion including noncontact vision-based

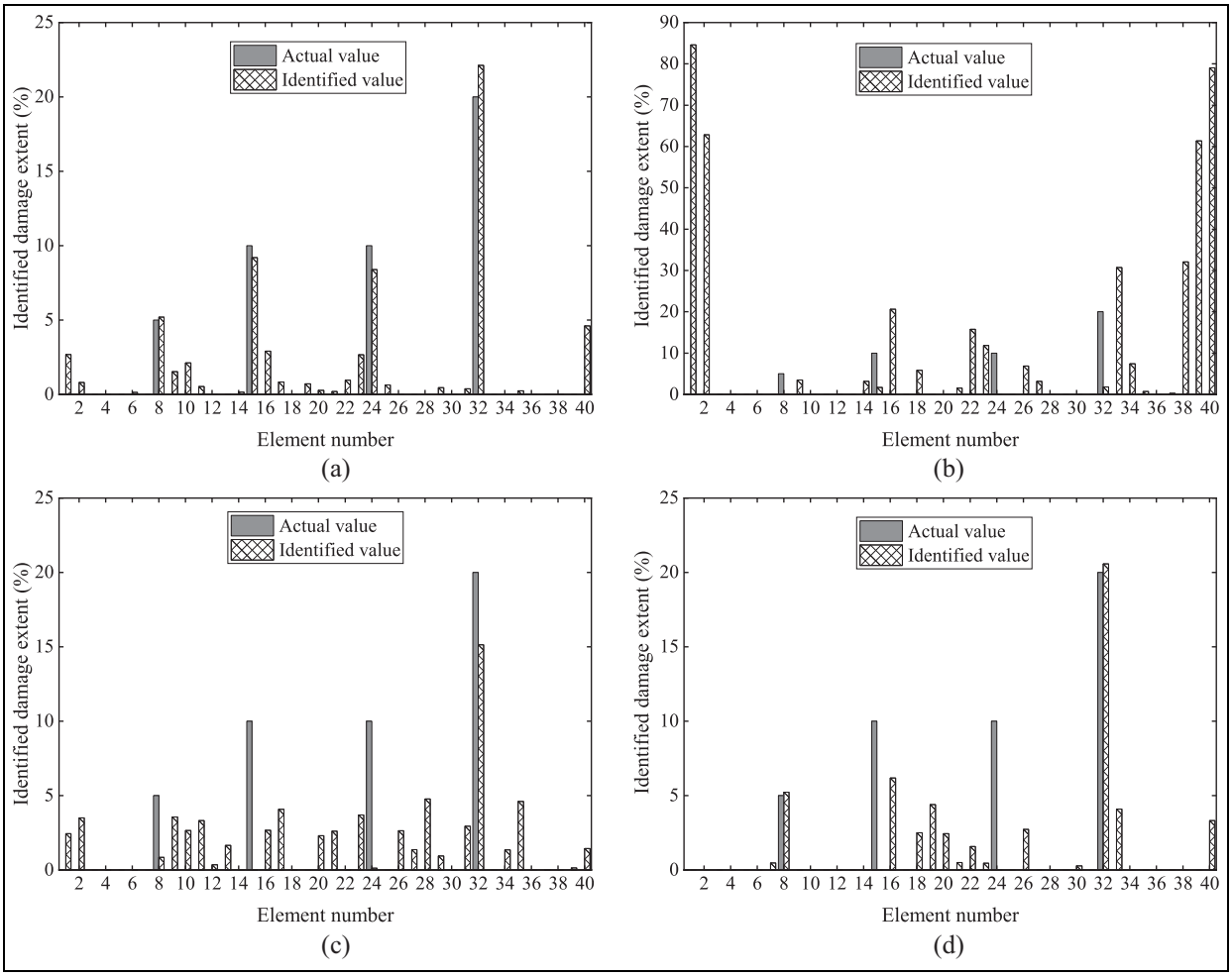

Figure 22. Damage results with different sensor placement configurations under 10% noise: (a) case 3(a), (b) case (3b), (c) case 3(c), and (d) case 3(d).

displacement measurement, accelerations, strains measurement from contact sensors for structural damage identification could be investigated in the future.

Acknowledgements

The author(s) would like to thank the anonymous reviewers for their detailed and fruitful remarks.

Declaration of conflicting interests

The author(s) declared no potential conflicts of interest with respect to the research, authorship, and/or publication of this article.

Funding

The author(s) disclosed receipt of the following financial support for the research, authorship, and/or publication of this article: National Key R&D Program of China (2021YFE0112200), the Japan Society for Promotion of Science (Kakenhi No. 18K04438), and the Tohoku Institute of Technology research Grant, the Postgraduate Research&Practice Innovation Program of Jiangsu Province (KYCX23_0273) the Project of Industry Foresight and Key Core Technologies (Grant No. BE2021021). These financial supports are sincerely appreciated.

ORCID iDs

Chunfeng Wan https://orcid.org/0000-0002-4236-6428
Jianfei Kang https://orcid.org/0000-0003-1205-747X
Liyu Xie https://orcid.org/0000-0001-5777-0645

References

1. Fan W and Qiao P. Vibration-based damage identification methods: a review and comparative study. *Struct Health Monit* 2011; 10(1): 83–111.
2. Feng K, González A and Casero M. A kNN algorithm for locating and quantifying stiffness loss in a bridge from the forced vibration due to a truck crossing at low speed. *Mech Syst Signal Process* 2021; 154: 107599.
3. Greś S, Döhler M and Mevel L. Statistical model-based optimization for damage extent quantification. *Mech Syst Signal Process* 2021; 160: 107894.

4. Gomes GF and Giovani RS. An efficient two-step damage identification method using sunflower optimization algorithm and mode shape curvature (MSDBI–SFO). *Eng Comput* 2020; 38(5): 1–20.
5. Seyedpoor SM and Yazdanpanah O. An efficient indicator for structural damage localization using the change of strain energy based on static noisy data. *Appl Math Model* 2014; 38(9–10): 2661–2672.
6. Carrella A and Ewins DJ. Identifying and quantifying structural nonlinearities in engineering application from measured frequency response functions. *Mech Syst Signal Process* 2011; 25(3): 1011–1027.
7. Chu SY and Lo SC. Application of the on-line recursive least-squares method to perform structural damage assessment. *Struct Control Health Monit* 2011; 18(3): 241–264.
8. Xue ST, Wen B, Huang R, et al. Parameter identification for structural health monitoring based on Monte Carlo method and likelihood estimate. *Int J Distrib Sens Netw* 2018; 14(7): 1550147718786888.
9. Xie LY, Zhou ZW, Zhao L, et al. Parameter identification for structural health monitoring with extended Kalman filter considering integration and noise effect. *Appl Sci-Basel* 2018; 8(12): 2480.
10. Wan ZM, Wang T, Li SD, et al. A modified particle filter for parameter identification with unknown inputs. *Struct Control Health Monit* 2018; 25(12): e2268.
11. Ni PH, Yin Z, Han Q, et al. Output-only structural identification with random decrement technique. *Structures* 2023; 51: 55–66.
12. Yang ZC, Yu ZF and Sun H. On the cross correlation function amplitude vector and its application to structural damage detection. *Mech Syst Signal Process* 2007; 21(7): 2918–2932.
13. Zhang GC, Wan CF, Xiong XB, et al. Output-only structural damage identification using hybrid Jaya and differential evolution algorithm with reference-free correlation functions. *Measurement* 2022; 199: 111591.
14. Zhang L, Feng DM and Wu G. Simultaneous identification of bridge damage and vehicle parameters based on bridge strain responses. *Struct Control Health Monit* 2022; 29(6): e2945.
15. He J, Zhang XX and Xu B. Identification of structural parameters and unknown inputs based on revised observation equation: approach and validation. *Int J Struc Stab Dyn* 2019; 19(12): 1950156.
16. Zhang XX, He J, Hua XG, et al. Simultaneous identification of time-varying parameters and external loads based on extended Kalman filter: approach and validation. *Struct Control Health Monit* 2023; 2023: 8379183.
17. Jayalakshmi V and Rao ARM. Simultaneous identification of damage and input dynamic force on the structure for structural health monitoring. *Struct Multi-Discip Optim* 2017; 55: 2211–2238.
18. Zhang GC, Wan CF, Xie LY, et al. Structural damage identification with output-only measurements using modified Jaya algorithm and Tikhonov regularization method. *Smart Struct Syst* 2023; 31(3): 229–245.
19. Yang J and Peng Z. A new convolutional neural network-based framework and data construction method for structural damage identification considering sensor placement. *Meas Sci Technol* 2023; 34(7): 075008.
20. Chen C, Tang L, Lu Y, et al. Reconstruction of long-term strain data for structural health monitoring with a hybrid deep-learning and autoregressive model considering thermal effects. *Eng Struct* 2023; 285: 116063.
21. Fan G, Li J and Hao H. Dynamic response reconstruction for structural health monitoring using densely connected convolutional networks. *Struct Health Monit* 2021; 20(4): 1373–1391.
22. Li J and Hao H. Substructure damage identification based on wavelet-domain response reconstruction. *Struct Health Monit* 2014; 13(4): 389–405.
23. Zhu HP, Mao L and Weng S. A sensitivity-based structural damage identification method with unknown input excitation using transmissibility concept. *J Sound Vib* 2014; 333(26): 7135–7150.
24. Ni PH, Li Q, Han Q, et al. Substructure approach for Bayesian probabilistic model updating using response reconstruction technique. *Mech Syst Signal Process* 2023; 183: 109624.
25. Chen ZP and Yu L. A novel PSO-based algorithm for structural damage detection using Bayesian multi-sample objective function. *Struct Eng Mech* 2017; 63(6): 825–835.
26. Ding ZH, Li J, Hao H, et al. Structural damage identification with uncertain modelling error and measurement noise by clustering based tree seeds algorithm. *Eng Struct* 2019; 185: 301–314.
27. Zhou HY, Zhang GC, Wang XJ, et al. A hybrid identification method on butterfly optimization and differential evolution algorithm. *Smart Struct Syst* 2020; 26(3): 345–360.
28. Ghiasi R, Fathnejat H and Torkzadeh P. A three-stage damage detection method for large-scale space structures using forward substructuring approach and enhanced bat optimization algorithm. *Eng Comput* 2019; 35: 857–874.
29. Rao R. Jaya: a simple and new optimization algorithm for solving constrained and unconstrained optimization problems. *Int J Ind Eng Comp* 2016; 7(1): 19–34.
30. Zhang GC, Wan CF, Xue ST, et al. A global-local hybrid strategy with adaptive space reduction search method for structural health monitoring. *Appl Math Model* 2023; 121: 231–251.
31. Ding ZH, Li J and Hao H. Structural damage identification using improved Jaya algorithm based on sparse regularization and Bayesian inference. *Mech Syst Signal Process* 2019; 132: 211–231.
32. Ding ZH, Hou RR and Xia Y. Structural damage identification considering uncertainties based on a Jaya algorithm with a local pattern search strategy and L0.5 sparse regularization. *Eng Struct* 2022; 261, 114312.
33. Kaveh A, Hosseini SM and Zaerreza A. Improved Shuffled Jaya algorithm for sizing optimization of skeletal structures with discrete variables. *Structures* 2021; 29: 107–128.
34. Wu RT and Jahanshahi MR. Data fusion approaches for structural health monitoring and system identification:

past, present, and future. *Struct Health Monit* 2020; 19(2): 552–586.
35. Zhao Y, Xu B, Deng B, et al. Various damper forces and dynamic excitation nonparametric identification with a double Chebyshev polynomial using limited fused measurements. *Measurement* 2022; 193: 110940.
36. Zhang CD and Xu YL. Structural damage identification via multi-type sensors and response reconstruction. *Struct Health Monit* 2016; 15(6): 715–729.
37. Jeong S, Kim EJ, Park JW, et al. Data fusion-based damage identification for a monopile offshore wind turbine structure using wireless smart sensors. *Ocean Eng* 2020; 195: 106728.
38. Wang XJ, Chen F, Zhou HY, et al. Structural damage detection based on cross-correlation function with data fusion of various dynamic measurements. *J Sound Vib* 2022; 541: 117373.
39. Li XY and Law SS. Condition assessment of structures under ambient white noise excitation. *AIAA J* 2008; 46(6): 1395–1404.
40. Norrie DH and de Vries G. *An introduction to finite element analysis*. Academic Press, New York, 1978.
41. Weber B, Paultre P and Proulx J. Structural damage detection using nonlinear parameter identification with Tikhonov regularization. *Struct Control Health Monit* 2007; 14(3): 406–427.
42. Yuen KV. *Bayesian methods for structural dynamics and civil engineering*. Singapore: John Wiley & Sons, 2010.
43. Samma H, Mohamad-Saleh J, Suandi SA, et al. Q-learning-based simulated annealing algorithm for constrained engineering design problems. *Neural Comput Appl* 2020; 32: 5147–5161.
44. Ding ZH, Li LF, Wang XY, et al. Vibration-based FRP debonding detection using a Q-learning evolutionary algorithm. *Eng Struct* 2023; 275: 115254.
45. Kaveh A, Dadras Eslamlou A, Rahmani P, et al. Optimal sensor placement in large-scale dome trusses via Q-learning-based water strider algorithm. *Struct Control Health Monit* 2022; 29(7): e2949.
46. Huynh TN, Do DTT and Lee J. Q-Learning-based parameter control in differential evolution for structural optimization. *Appl Soft Comput* 2021; 107: 107464.
47. Pathirage CSN, Li J, Li L, et al. Structural damage identification based on autoencoder neural networks and deep learning. *Eng Struct* 2018; 172: 13–28.
48. Dinh-Cong D, Vo-Duy T, Ho-Huu V, et al. An efficient multi-stage optimization approach for damage detection in plate structures. *Adv Eng Softw* 2017; 112: 76–87.